## Further Development of a Time Domain Boundary Integral Equation Method for Aeroacoustic Scattering Computations

Fang Q. Hu\*

Old Dominion University, Norfolk, Virginia, 23529

Recently, a stable time domain boundary integral equation for the acoustic convective wave equation has been formulated and an efficient numerical solution has been proposed. The time domain boundary integral equation solver has several distinct advantages. For instances, scattering solutions at all frequencies can be obtained within one single time domain computation. Furthermore, broadband sources and time dependent transient signals can be simulated and studied directly, and it can be readily coupled with a nonlinear CFD simulation where many frequencies are generated. In the present paper, further developments of the time domain boundary integral equation solver are reported. A Fourier analysis for the general interpolation problem is formulated. In the literature, the temporal basis functions used in March-On-in-Time (MOT) schemes have been largely limited to low-order shifted Lagrange basis functions. The current work seeks an improvement on the temporal basis function. Based on the Fourier analysis, the resolutions of various temporal basis functions are quantified. Then, optimized basis functions that have significantly extended resolution in the Fourier frequency space are proposed. Substantial improvements in accuracy and efficiency of the proposed optimal high-resolution temporal basis functions for time domain integral equations are demonstrated by numerical examples. The use of optimized basis functions keeps the error low for a larger range in the frequency space. Conversely, for a given range of frequency of interest, a larger time step can used with the optimized temporal basis functions, resulting in a significant increase in computational efficiency and, at the same time, reduction in memory requirement. The time domain boundary integral equation solver is further applied to the problem of scattering by a flat plate. Computed results are compared with the experimental measurements.

## I. Introduction

In assessing noise shielding effects of an aircraft body or its components, there is a need to effectively and accurately calculate sound scattering by an acoustically large body at mid to high frequencies. While it is well-known that acoustic scattering problem can be formulated as boundary integral equations, both in the time domain and in the frequency domain, a vast majority of research and computational solvers, however, have been done in the frequency domain. As noted in many studies on time domain solutions, there are several distinct advantages that are afforded by the time domain formulation. For instances, scattering solutions at all frequencies can be obtained within one single time domain computation. Furthermore, broadband sources and time dependent transient signals can be simulated and studied directly, and it is more natural to couple a nonlinear CFD simulation with time domain solver than one in the frequency domain where many frequencies are generated.

<sup>\*</sup>Professor, Department of Mathematics and Statistics, AIAA Associate Fellow

In the past the development of time domain approach has been hindered by two major difficulties. The first was the intrinsic instability in the early time domain formulations due to the presence of resonant frequencies which are bound to exist in time domain calculations. The second was the formidably high computational costs in solving the time domain integral equation. Significant progresses have been made in recent years in resolving these two major difficulties. Stability can now be achieved by using a Burton-Miller type formulation or Convolution Quadratures.<sup>7,10,17,18,24,25,31</sup> And there are recent developments where computational complexity can be reduced from  $O(N_tN^2)$  to  $O(N_tN\log^2 N)$  where N is the total number of unknowns, and  $N_t$  is the total number of time steps.<sup>11,19,26</sup> For instance, for March-On-in-Time (MOT) schemes, the recently developed Plane Wave Time Domain (PWTD) algorithm can be used to accelerate the far interactions,<sup>11</sup> akin to the Fast Multipole Methods in the frequency domain.<sup>13-15</sup> With these breakthroughs, as well as the advances in computational power and new computing architectures, it is easy to foresee an increase in the application of time domain integral equations in the future.

Recently, a formulation of stable time domain boundary integral equation for the acoustic convective wave equation has been given in [19] based on a Burton-Miller type reformulation of the well-known Kirchhoff integral relation. An efficient Time Domain Propagation and Distribution (TDPD) algorithm has been developed, based on the delay- and amplitude-compensated acoustic field and a simplified multi-level Cartesian Non-uniform Grid Time Domain Algorithm (CNGTDA).<sup>19,26</sup> In [19], the computation is further accelerated by General Purpose GPU computing, making it feasible for practical applications to scattering solutions with several millions of unknowns.

In the present paper, further developments of the time domain boundary integral equation solver are reported. Specifically, advances in two areas are presented. In the first area, Sections 2-5, a systematic analysis of the temporal basis functions used in MOT schemes is carried out. In the literature, with a few exceptions(e.g., [12, 32, 33]), the temporal basis functions used in MOT schemes have been largely limited to low-order shifted Lagrange basis functions. The current work seeks an improvement on the temporal basis function. A Fourier analysis for the general interpolation problem is formulated. Based on the Fourier analysis, the resolutions of various temporal basis functions are quantified. Then, optimized basis functions that have significantly extended resolution in the Fourier frequency space are proposed. Substantial improvements in accuracy and efficiency of the proposed optimal high-resolution temporal basis functions for time domain integral equations are demonstrated by numerical examples.

In the second area, Section 6, the time domain boundary integral equation solver is applied to the problem of scattering by a flat plate. The computed results are compared with the experimental measurements carried out in a NASA report.<sup>1</sup> Concluding remarks are given in section 7.

#### II. Temporal basis functions

#### A. Time domain integral equation

As shown in [19], the time domain boundary integral equation for acoustic scattering is

$$2\pi p(\mathbf{r}_s',t) = \frac{1}{c^2} \int_{V} \frac{1}{\bar{R}} q(\mathbf{r},t_R) d\mathbf{r} + \int_{S} \left[ \left( 1 - M_n^2 \right) G_0 \frac{\partial p}{\partial n} (\mathbf{r}_s, t_R) - \frac{\partial G_0}{\partial \bar{n}} p(\mathbf{r}_s, t_R) \right]$$

$$-M_n G_0 \left( \mathbf{M}_T \cdot \nabla p(\mathbf{r}_s, t_R) \right) + \frac{1}{c\alpha^2} G_0 \left( \frac{\partial \bar{R}}{\partial \bar{n}} - \alpha^2 M_n \right) \frac{\partial p}{\partial t} (\mathbf{r}_s, t_R) d\mathbf{r}_s$$

$$(1)$$

where  $q(\mathbf{r},t)$  represents the source term and  $t_R$  is the retarded time defined as

$$t_R = t + \beta \cdot (\mathbf{r}_s' - \mathbf{r}_s) - \bar{R}/c\alpha^2 \tag{2}$$

and the parameters appeared in (1) are

$$\alpha = \sqrt{1 - (U/c)^2}, \ \beta = \frac{U}{c^2 - U^2} = \frac{U}{c^2 \alpha^2} = \frac{M}{c\alpha^2}, \ \bar{n} = n - M_n M$$

$$G_0 = \frac{1}{\bar{R}}$$
, and  $\bar{R} = \sqrt{(x_s - x_s')^2 + \alpha^2(y_s - y_s')^2 + \alpha^2(z_s - z_s')^2}$  (3)

Further details on (1) are referred to [19].

To discretize the integral equation (1), the integral surface S is divided into boundary elements and the numerical solution on the surface is expressed as

$$p(\mathbf{r}_s, t) = \sum_{i=1}^{N_e} p_i(t)\phi_i(\mathbf{r}_s)$$
(4)

in which  $N_e$  is the total number of surface nodes and  $\phi_i(\mathbf{r}_s)$  is the surface basis function for the *i*-th node on the surface. In (4),  $p_i(t)$  denotes the nodal value as a function of t for the *i*-th node. This temporal dependence is often constructed through a use of temporal basis function  $\psi_j(t)$  as

$$p_{i}(t) = \sum_{j=0}^{N_{t}} u_{i}^{j} \psi_{j}(t)$$
 (5)

where  $N_t$  is the total number of time steps and  $u_i^j$  is the value of solution of the *i*-th node at time  $t_j$ . That is, we have

$$p_i(t_j) = u_i^j \tag{6}$$

Here, we assume that the temporal grid is created with a uniform time step  $\Delta t$  and

$$t_j = t_0 + j\Delta t \tag{7}$$

where  $t_0$  is an arbitrary time for j = 0.

In the collocation March-On-in-Time (MOT) approach, the integral equation (1) is enforced progressively at each time step. By substituting (4) into (1), assuming for the moment  $\frac{\partial p}{\partial n} = 0$  and M = 0 for simplicity, and evaluating at a collocation time  $t_n$ , we get

$$2\pi p(\mathbf{r}'_s, t_n) = \frac{1}{c^2} \int_V \frac{1}{R} q(\mathbf{r}'_s, t'_R) d\mathbf{r} - \int_S \left[ \frac{\partial G_0}{\partial \bar{n}} \sum_{i=1}^N p_i(t'_R) \phi_i(\mathbf{r}_s) - \frac{1}{c} G_0 \left( \frac{\partial R}{\partial \bar{n}} \right) \sum_{i=1}^N \frac{dp_i}{dt} (t'_R) \phi_i(\mathbf{r}_s) \right] d\mathbf{r}_s$$

or

$$2\pi p(\mathbf{r}_{s}',t_{n}) = \frac{1}{c^{2}} \int_{V} \frac{1}{R} q(\mathbf{r}_{s}',t_{R}') d\mathbf{r} - \sum_{i=1}^{N} \int_{S_{i}} \left[ \frac{\partial G_{0}}{\partial \bar{n}} p_{i}(t_{R}') - \frac{1}{c} G_{0} \left( \frac{\partial R}{\partial \bar{n}} \right) \frac{dp_{i}}{dt}(t_{R}') \right] \phi_{i}(\mathbf{r}_{s}) d\mathbf{r}_{s}$$
(8)

where  $S_i$  denotes the element for which the surface basis function  $\phi_i(r_s)$  is non-zero and

$$t_R' = t_n + \beta \cdot (\mathbf{r}_s' - \mathbf{r}_s) - \bar{R}/c\alpha^2 \tag{9}$$

Using the discretization stipulated in (4) and (5), equation (8) can be cast into an algebraic iteration scheme of the form

$$\mathbf{B}_0 \mathbf{u}^n = \mathbf{q}^n - \sum_{k=1}^{k_M} \mathbf{B}_m \mathbf{u}^{n-k} \tag{10}$$

where  $u^n$  denotes the vector of all coefficients  $u_i^n$  at time level  $t_n$ , and  $k_M$  denotes the limit for index k.

As illustrated in equation (8), to solve the integral equation, there is a need to compute  $p_i(t'_R)$  and  $\frac{dp_i}{dt}(t'_R)$  at a time determined by  $t'_R$  in (9), the retarded time between  $r_s$  and  $r'_s$ . Furthermore, when equation (8) is cast into a Burton-Miller type formulation, there is also a need to compute the second time derivative  $\frac{d^2p_i}{dt^2}(t'_R)$ . In what follows, we discuss in detail the computational method for these values under the framework given in expression (5).

#### B. Conventional one-sided shifted Lagrange basis function

In most MOT formulations, the temporal basis function  $\psi_j(t)$  is assumed to be of the same form for all time nodes and expressed as in the following,

$$\psi_{j}(t) = \Psi(t - t_{j}) = \begin{cases}
\bar{\Psi}_{0}(\tau) & -\Delta t < t - t_{j} \leq 0 \\
\bar{\Psi}_{-1}(\tau) & 0 < t - t_{j} \leq \Delta t \\
\bar{\Psi}_{-2}(\tau) & \Delta t < t - t_{j} \leq 2\Delta t \\
\dots & \dots \\
\bar{\Psi}_{-m}(\tau) & (m - 1)\Delta t < t - t_{j} \leq m\Delta t \\
0 & \text{other}
\end{cases}$$
(11)

in which m is the chosen order of basis function and  $\bar{\Psi}_{\ell}(\tau)$ ,  $\tau = (t - t_j)/\Delta t$ , is a shifted Lagrange polynomial formed as follows:

$$\bar{\Psi}_{\ell}(\tau) = \frac{\prod_{i=-m, i \neq \ell}^{0} [-\tau + (i-\ell)]}{\prod_{i=-m, i \neq \ell}^{0} [(i-\ell)]}, \quad \ell = -m, ..., 0$$
(12)

For convenience of discussion,  $\bar{\Psi}_{\ell}(\tau)$  will be referred to as  $\tau$ -normalized basis functions. Equation (12) yields a temporal basis function that is a piecewise m-th order polynomial. For instances, the popular second-, third- and fouth-order shifted Lagrange basis functions are

Second order:

$$\bar{\Psi}(\tau) = \begin{cases}
1 + \frac{3}{2}\tau + \frac{1}{2}\tau^2 & -1 < \tau \le 0 \\
1 - \tau^2 & 0 < \tau \le 1 \\
1 - \frac{3}{2}\tau + \frac{1}{2}\tau^2 & 1 < \tau \le 2 \\
0 & \text{other}
\end{cases}$$
(13)

Third order:

$$\bar{\Psi}(\tau) = \begin{cases}
1 + \frac{11}{6}\tau + \tau^2 + \frac{1}{6}\tau^3 & -1 < \tau \le 0 \\
1 + \frac{1}{2}\tau - \tau^2 - \frac{1}{2}\tau^3 & 0 < \tau \le 1 \\
1 - \frac{1}{2}\tau - \tau^2 + \frac{1}{2}\tau^3 & 1 < \tau \le 2 \\
1 - \frac{11}{6}\tau + \tau^2 - \frac{1}{6}\tau^3 & 2 < \tau \le 3 \\
0 & \text{other}
\end{cases} \tag{14}$$

Fourth order:

$$\bar{\Psi}(\tau) = \begin{cases}
1 + \frac{25}{12}\tau + \frac{35}{24}\tau^2 + \frac{5}{12}\tau^3 + \frac{1}{24}\tau^4 & -1 < \tau \le 0 \\
1 + \frac{5}{6}\tau - \frac{5}{6}\tau^2 - \frac{5}{6}\tau^3 - \frac{1}{6}\tau^4 & 0 < \tau \le 1 \\
1 - \frac{5}{4}\tau^2 + \frac{1}{4}\tau^4 & 1 < \tau \le 2 \\
1 - \frac{5}{6}\tau - \frac{5}{6}\tau^2 + \frac{5}{6}\tau^3 - \frac{1}{6}\tau^4 & 2 < \tau \le 3 \\
1 - \frac{25}{12}\tau + \frac{35}{24}\tau^2 - \frac{5}{12}\tau^3 + \frac{1}{24}\tau^4 & 3 < \tau \le 4 \\
0 & \text{other}
\end{cases} \tag{15}$$

Because the temporal basis function (11) has a finite support in time, the contribution from any node i to the solution at location  $\mathbf{r}'_s$  and at collocation time  $t_n$ , as appeared in (8), reduces to a summation of m+1 terms, namely,

$$p_i(t_R') = \sum_{j=0}^{N_t} u_i^j \psi_j(t_R') = u_i^J \Psi(t_R' - t_J) + u_i^{J-1} \Psi(t_R' - t_{J-1}) + u_i^{J-2} \Psi(t_R' - t_{J-2}) + \dots + u_i^{J-m} \Psi(t_R' - t_{J-m})$$
 (16)

or, in terms of the  $\tau$ -normalized basis functions,

$$p_{i}(t'_{R}) = u_{i}^{J}\bar{\Psi}_{0}\left(\frac{t'_{R} - t_{J}}{\Delta t}\right) + u_{i}^{J-1}\bar{\Psi}_{-1}\left(\frac{t'_{R} - t_{J-1}}{\Delta t}\right) + u_{i}^{J-2}\bar{\Psi}_{-2}\left(\frac{t'_{R} - t_{J-2}}{\Delta t}\right) + \dots + u_{i}^{J-m}\bar{\Psi}_{-m}\left(\frac{t'_{R} - t_{J-m}}{\Delta t}\right)$$
(17)

where

$$t_J = t_0 + J\Delta t$$
,  $J = \text{ceiling}\left(\frac{t_R' - t_0}{\Delta t}\right)$ , and  $t_{J-1} < t_R' \le t_J$  (18)

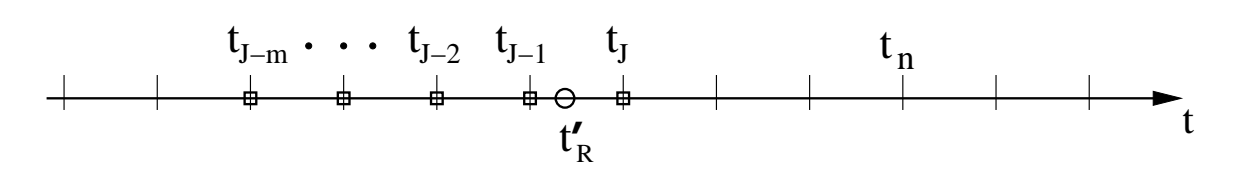


Figure 1. A schematic showing the grid in time and the temporal interpolation stencils resulted from one-sided basis functions shown in (11).  $t_n$  is the current time step and  $t'_R$  is the time at which interpolation is required.

Equation (16) shows that a use of the basis function of the form (11) results in an interpolation for  $p_i(t_R')$  from the values on nodal points  $t_{J-m}, t_{J-m+1}, \cdots, t_{J-1}, t_J$ . In other words, using the basis functions of the type shown in (11) results in an interpolation that is completely one-sided. While, due to causality, this one-sidedness is necessary when  $t_J$ , determined by (18) is the same as the current collocation time step  $t_n$ . It is, however, un-necessary when  $t_J$  is a time that is a few time steps earlier than  $t_n$ , as illustrated in Figure 1. In such cases, an interpolation that uses more points to the right of  $t_J$  is possible, as will be discussed next. The benefits of using two-sided interpolations will be further analyzed in Section 3.

#### C. General two-sided Lagrange temporal basis functions

A general interpolation problem is to find an approximation at any given location based on the values known on a specified grid. As discussed in the previous section, it is possible to use two-sided interpolation for computing  $p_i(t_R')$ ,  $\frac{dp_i}{dt}(t_R')$ , or  $\frac{d^2p_i}{dt^2}(t_R')$ , when  $t_R'$  is a few time steps earlier than the current collocation time  $t_n$ . We consider a general interpolation problem for the value at a point located at  $t' = t_j - \eta \Delta t$ ,  $0 \le \eta < 1$ , using a stencil from  $t_{j-M}$  to  $t_{j+N}$ :

$$p(t') = \sum_{\ell=-M}^{N} S_{\ell}(\eta) u^{j+\ell}$$

$$\tag{19}$$

as show in Figure 2. For brevity, the subscript i, indication for the i-th node, will be dropped in the following discussion. Here,  $u^j$  denotes the values known on the grid formed by  $t_j$  and  $S_{\ell}(\eta)$  are the coefficients of interpolation scheme for the value at a point t' located between  $t_{j-1}$  and  $t_j$ . If the Lagrange interpolation polynomials are used, we have simply

$$S_{\ell}(\eta) = \frac{\prod_{\ell'=-M, \ell' \neq \ell}^{N} (t' - t_{j+\ell'})}{\prod_{\ell'=-M, \ell' \neq \ell}^{N} (t_{j+\ell} - t_{j+\ell'})} = \frac{\prod_{\ell'=-M, \ell' \neq \ell}^{N} (\ell' + \eta)}{\prod_{\ell'=-M, \ell' \neq \ell}^{N} (\ell' - \ell)}$$
(20)

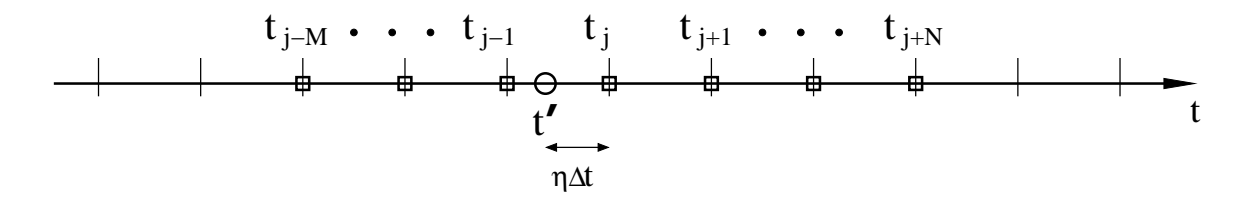


Figure 2. A schematic diagram for a general interpolation stencil along the time grid.

It is straightforward to see that when  $S_{\ell}(\eta)$  in (19) are converted to temporal basis functions and are expressed similarly to that in (11), we have the equivalent  $\tau$ -normalized basis functions as

$$\bar{\Psi}_{\ell}(\tau) = S_{\ell}(-\tau - \ell), \quad \ell = -M, ..., N$$
 (21)

where  $\tau$  and  $\eta$  are related as

$$\tau = \frac{t' - t_{j+\ell}}{\Delta t} = -\eta - \ell \tag{22}$$

Conversely, we have

$$S_{\ell}(\eta) = \bar{\Psi}_{\ell}(-\eta - \ell) \tag{23}$$

The explicit forms for the  $\tau$ -normalized basis functions derived from the two-sided Lagrange interpolation polynomials (20) are given in Appendix A, tables 1-3.

In the formulations of time domain integral equations, interpolations for the derivatives with respect to time (up to second-oder when the Burton-Miller type formulation is used) are also required. They can be computed as

$$\frac{dp}{dt}(t') = -\frac{1}{\Delta t} \sum_{\ell=-M}^{N} S'_{\ell}(\eta) u^{j+\ell}$$
(24)

$$\frac{d^2p}{dt^2}(t') = \frac{1}{\Delta t^2} \sum_{\ell=-M}^{N} S_{\ell}''(\eta) u^{j+\ell}$$
 (25)

where  $S'_{\ell}(\eta)$  and  $S''_{\ell}(\eta)$  are respectively the first and second derivatives with respect to  $\eta$ .

## III. Fourier analysis of temporal basis functions

Obviously, the accuracy of a particular interpolation scheme can be assessed in many different ways. In this section, we analyze the error of temporal interpolation scheme (19) in the Fourier frequency space. For spatial interpolation schemes, wave number analysis has been conducted earlier in [29, 30]. In the current work, the analysis is carried out in the temporal dimension.

For a grid function  $u^j$ , defined on a uniform grid of  $t_i = t_0 + j\Delta t$ , it has a discrete Fourier transform,

$$\hat{u}(\omega) = \Delta t \sum_{j=-\infty}^{\infty} u^j e^{-it_j \omega}$$
(26)

and the inverse as

$$u^{j} = \frac{1}{2\pi} \int_{-\pi/\Delta t}^{\pi/\Delta t} e^{it_{j}\omega} \hat{u}(\omega) d\omega$$
 (27)

Equations (26) and (27) indicate that the spectrum for  $u^j$ , when the grid is infinitely wide, would be one that is continuous but limited to  $\frac{\pi}{\Delta t}$ , the Nyquist limit. We are interested in an interpolation scheme that will preserve the spectrum  $\hat{u}(\omega)$  as much as possible.

It is well-known that a special interpolation function called cardinal interpolation, denoted as  $u^{I}(t)$ , that recovers the full spectrum  $\hat{u}(\omega)$  as defined in (26) and (27) can be constructed as follows,<sup>28</sup>

$$u^{I}(t) = \frac{1}{2\pi} \int_{-\pi/\Delta t}^{\pi/\Delta t} e^{it\omega} \hat{u}(\omega) d\omega = \frac{1}{2\pi} \int_{-\pi/\Delta t}^{\pi/\Delta t} e^{it\omega} \left( \Delta t \sum_{j=-\infty}^{\infty} u^{j} e^{-it_{j}\omega} \right) d\omega$$

$$= \frac{\Delta t}{2\pi} \sum_{j=-\infty}^{\infty} u^{j} \int_{-\pi/\Delta t}^{\pi/\Delta t} e^{it\omega} e^{-it_{j}\omega} d\omega = \frac{\Delta t}{2\pi} \sum_{j=-\infty}^{\infty} u^{j} \int_{-\pi/\Delta t}^{\pi/\Delta t} e^{i(t-t_{j})\omega} d\omega$$

$$= \sum_{j=-\infty}^{\infty} u^{j} \frac{\sin\left[ \left( \frac{t-t_{j}}{\Delta t} \right) \pi \right]}{\pi \left( \frac{t-t_{j}}{\Delta t} \right)} = \sum_{j=-\infty}^{\infty} u^{j} \operatorname{sinc}\left( \frac{t-t_{j}}{\Delta t} \pi \right)$$
(28)

Clearly, by (28), we have

$$u^I(t_j) = u^j$$

and its Fourier transform

$$\begin{split} \hat{u}^I(\omega) &= \int_{-\infty}^{\infty} u^I(t) e^{-i\omega t} dt = \int_{-\infty}^{\infty} \left( \int_{-\pi/\Delta t}^{\pi/\Delta t} e^{it\omega'} \hat{u}(\omega') d\omega' \right) e^{-i\omega t} dt \\ &= \int_{-\pi/\Delta t}^{\pi/\Delta t} \left( \int_{-\infty}^{\infty} e^{it\omega'} e^{-i\omega t} dt \right) \hat{u}(\omega') d\omega' = \int_{-\pi/\Delta t}^{\pi/\Delta t} \left( \int_{-\infty}^{\infty} e^{-i\left[\omega-\omega'\right]t} dt \right) \hat{u}(\omega') d\omega' \\ &= \int_{-\pi/\Delta t}^{\pi/\Delta t} \delta \left( \omega - \omega' \right) e^{-it_0\omega'} \hat{u}(\omega') d\omega' = \begin{cases} \hat{u}(\omega), & |\omega\Delta t| < \pi \\ 0, & |\omega\Delta t| > \pi \end{cases} \end{split}$$

While the interpolation function  $u^{I}(t)$  by (28) preserves the full spectrum of  $u^{j}$ , its stencil is unfortunately infinitely wide.

We now consider the Fourier frequency space for the interpolation defined in (19). Following the definition of discrete Fourier transform in (26), the spectrum of the interpolated function p(t') computed on the grid  $t'_i = t_j - \eta \Delta t$  is

$$\hat{p}(\eta,\omega) = \Delta t \sum_{j=-\infty}^{\infty} p(t_j - \eta \Delta t) e^{-i(t_j - \eta \Delta t)\omega} = \Delta t \sum_{j=-\infty}^{\infty} \left( \sum_{j=-M}^{N} S_{\ell}(\eta) u^{j+\ell} \right) e^{-i(t_j - \eta \Delta t)\omega}$$

$$= \sum_{\ell=-M}^{N} S_{\ell}(\eta) \left( \Delta t \sum_{j=-\infty}^{\infty} u^{j+\ell} e^{-it_{j}\omega} \right) e^{i\eta\omega\Delta t} = e^{i\eta\omega\Delta t} \sum_{\ell=-M}^{N} \left[ S_{\ell}(\eta) e^{i\ell\omega\Delta t} \left( \Delta t \sum_{j=-\infty}^{\infty} u^{j+\ell} e^{-it_{j+\ell}\omega} \right) \right]$$

$$=e^{i\eta\omega\Delta t}\left(\sum_{\ell=-M}^{N}S_{\ell}(\eta)e^{i\ell\omega\Delta t}\right)\hat{u}(\omega) \tag{29}$$

The result in (29) shows that an interpolation scheme of the form given in (19) would modify the spectrum of the original data  $u^j$  by a factor of

$$F_0(\eta, \xi) = e^{i\eta\xi} \left( \sum_{\ell=-M}^N S_\ell(\eta) e^{i\ell\xi} \right)$$
 (30)

where  $\xi$  is the non-dimensional frequency,

$$\xi = \omega \Delta t \tag{31}$$

The ideal value for  $F_0(\eta, \xi)$  is of course unity for all  $\eta$  and  $\xi$ , and any deviation of  $F_0(\eta, \xi)$  from unity represents the error of interpolation measured in the Fourier frequency space. To facilitate the ensuing discussions, we introduce

$$E_0(\eta, \xi) = \sum_{\ell=-M}^{N} S_{\ell}(\eta) e^{i\ell\xi} - e^{-i\eta\xi}$$
(32)

as a measure for the error of interpolation in the frequency space. Clearly, we have the relation

$$E_0(\eta, \xi) = (F_0(\eta, \xi) - 1) e^{-i\eta\xi}$$
(33)

Furthermore, interpolation errors for the first and second time derivatives will be conveniently assessed by  $E_1(\eta, \xi)$  and  $E_2(\eta, \xi)$  respectively:

$$E_1(\eta, \xi) = \frac{dE_0}{d\eta}(\eta, \xi) = \sum_{\ell=-M}^{N} S'_{\ell}(\eta) e^{i\ell\xi} + i\xi e^{-i\eta\xi}$$
(34)

$$E_2(\eta, \xi) = \frac{d^2 E_0}{d\eta^2}(\eta, \xi) = \sum_{\ell=-M}^N S_\ell''(\eta) e^{i\ell\xi} + \xi^2 e^{-i\eta\xi}$$
(35)

Using the third order basis function (14) as an example, the interpolation error functions  $E_0(\eta, \xi)$ ,  $E_1(\eta, \xi)$  and  $E_2(\eta, \xi)$  are shown as contour plots in Figure 3. The magnitude of the errors obviously would depend on the values of  $\eta$  and  $\xi$ .

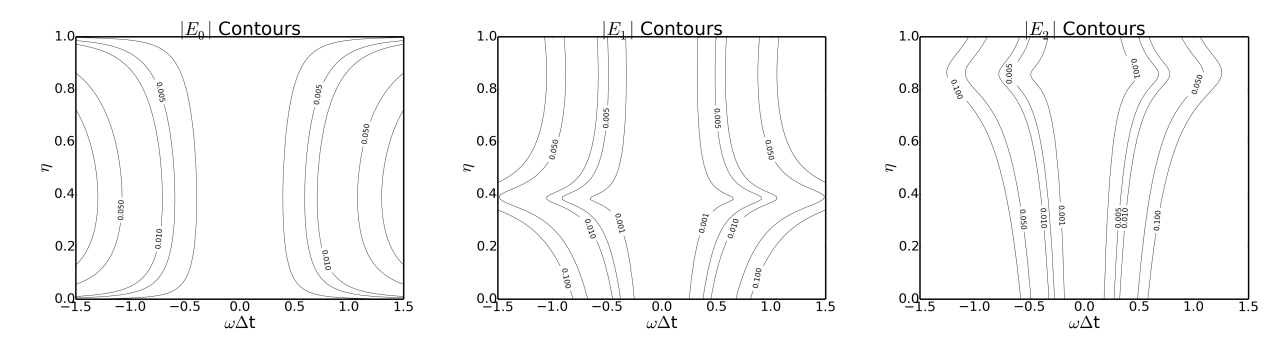


Figure 3. Contours of interpolation error functions  $E_0(\eta, \xi)$ ,  $E_1(\eta, \xi)$  and  $E_2(\eta, \xi)$ . Plotted are the errors for the third-order shifted Lagrange basis functions (14).

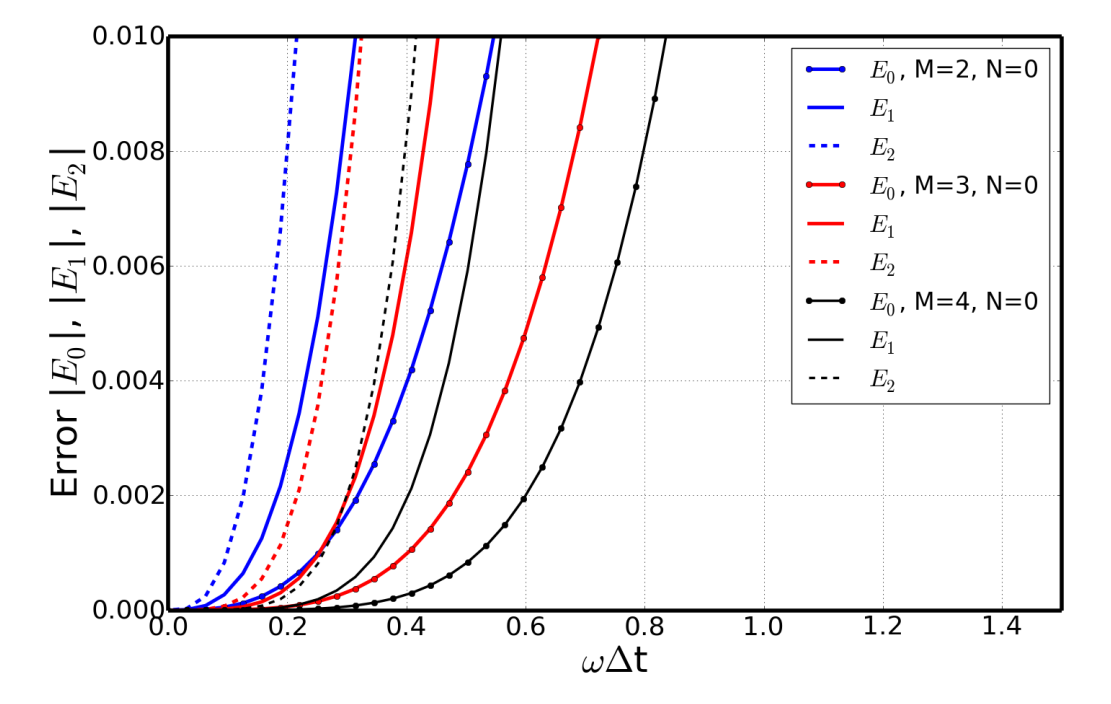


Figure 4. Interpolation error in Fourier frequency space for selected one-sided shifted Lagrange basis functions. Plotted are the maximum errors for  $0 \le \eta < 1$ .

In Figure 4, the interpolation error in the Fourier space as a function of the non-dimensional frequency  $\omega \Delta t$  is plotted for the second, third and fourth order one-sided shifted Lagrange basis functions. Plotted are the maximum values of  $|E_0(\eta,\xi)|$ ,  $|E_1(\eta,\xi)|$  and  $|E_2(\eta,\xi)|$  for all  $\eta$ ,  $0 \le \eta < 1$ , as a function of  $\xi$ . As expected, it is observed that the error is smaller when the order of basis functions is higher and, for the same order of basis functions, the error of interpolation for the second derivatives is larger than that for the first derivatives which is still larger than that for the value of function itself.

More important, Figure 4 yields an accuracy limit of the respective interpolation scheme in the frequency space. Using, for instances, 0.005 as a criterion on the maximum allowable error, the interpolation would be accurate for approximately  $\omega \Delta t \leq 0.15$ , 0.25, 0.35 and 0.45 for the second-, third-, fourth-order and fifth-order one-sided basis functions respectively. The accuracy limit defines the resolution associated with the temporal basis function. In other words, if  $T = 1/f = 2\pi/\omega$  is the wave period, the approximation up to the second time derivative will be considered accurate when the sampling in time is such that  $T/\Delta t \geq 42$ , 25, 18 and 14 respectively for the second-, third-, fourth- and fifth-order one-sided basis functions. This implies that, given a fixed time step size, a wider range of frequency is covered when higher order basis functions are used, or, equivalently, given a frequency of interest, a larger time step can be used. This clearly shows that, given sufficiently fine resolution in space, it is more efficient to use higher order basis functions.

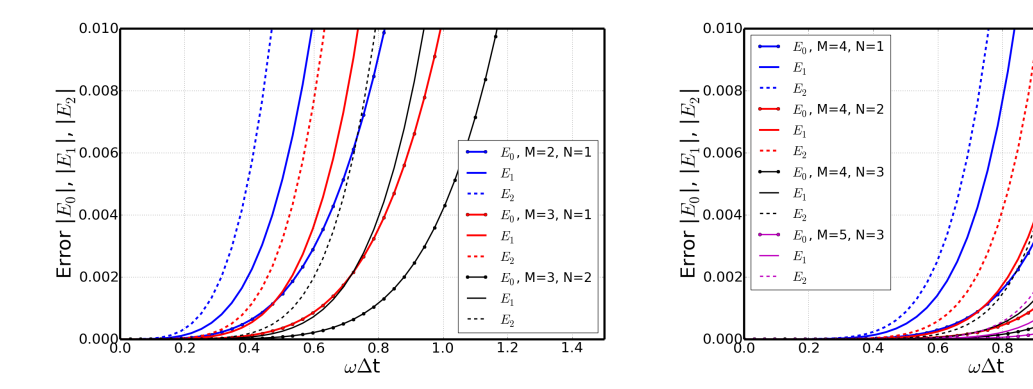


Figure 5. Interpolation errors in Fourier frequency space for selected two-sides Lagrange basis functions. Plotted are the maximum errors for  $0 \le \eta < 1$ .

In Figure 5, interpolation errors for two-sided interpolation schemes are plotted. It is seen that the errors are reduced as the interpolation stencil widens and as the order of basis function increases. However, more significant, comparing the cases of M3N0 with M2N1 and M4N0 with M3N1, even for the same number of stencils and the same order of basis functions, the two-sided interpolations have a much better resolution than the one-sided counter-parts.

Clearly, as far as the issue of accuracy is concerned, using two-sided interpolation is advantages. The two-sides interpolation with stencils from  $t_{J-M}$  to  $t_{J+N}$  is applicable whenever the following condition is met:

$$t_n - t_R' \ge N\Delta t \tag{36}$$

where  $t'_R$ , given by (9), is the time at which interpolation is required and J is that determined by (18).

#### IV. Optimization of temporal basis functions

Given a stencil of M + N + 1 points, from  $t_{j-M}$  to  $t_{j+N}$  as in Figure 2, a polynomial of order M + N can be uniquely determined, as was done and discussed in the previous section using the Lagrange polynomials.

However, instead of choosing the interpolation coefficients  $S_{\ell}(\eta)$ , or the resulting temporal basis function  $\bar{\Psi}_{\ell}(\tau)$ , to fit the highest possible order in  $\eta$ , or  $\tau$ , we can seek an optimization of the coefficients such that the interpolation error in the Fourier frequency space is minimized. The optimization procedure is similar

in spirit to those in [29, 30] for the spatial interpolations. The optimized schemes presented here, however, are valid for an arbitrary point in time and for up to the second derivative in time.

To this end, we will limit in this paper the form of  $S_{\ell}(\eta)$  to be a polynomial of  $\eta$  of degree M+N:

$$S_{\ell}(\eta) = \sum_{n=0}^{M+N} a_n^{(\ell)} \eta^n \tag{37}$$

The coefficients  $a_n^{(\ell)}$  are to be determined such that the following expression, which is the sum of interpolation error functions in the Fourier space,

OBJECTIVE: 
$$E = \int_{-\varepsilon_0}^{\xi_0} \int_0^1 \left[ |E_0(\eta, \xi)|^2 + |E_1(\eta, \xi)|^2 + |E_2(\eta, \xi)|^2 \right] d\eta d\xi$$
 (38)

is minimized. In (38),  $E_0(\eta, \xi)$ ,  $E_1(\eta, \xi)$  and  $E_2(\eta, \xi)$  are that given in (32), (34) and (35) respectively, and  $\xi_0$  is a chosen limit of the non-dimensional frequency for optimization.

In carrying out the optimization process, two additional conditions will also be considered. The first is an imposed order of interpolation m. By expanding (32) as a Taylor series in  $\xi$  and enforcing the equation up to order m, we get

$$\sum_{\ell=-M}^{N} S_{\ell}(\eta)\ell^{k} - (-\eta)^{k} = 0, \quad k = 0, 1, 2, ..., m$$
(39)

This condition ensures that the resulting optimized interpolation is accurate to order m in  $\eta$  and  $\xi$ . In terms of the coefficients  $a_n^{(\ell)}$  as defined in (37), the order condition (39) leads to the following constraint for optimization:

CONSTRAINT I: 
$$\sum_{\ell=-M}^{N} \ell^{k} a_{n}^{(\ell)} = (-1)^{k} \delta_{nk}, \quad n = 0, 1, ..., M + N, \quad k = 0, 1, ..., m$$
 (40)

In particular, when the highest possible order for (39) is enforced at m = M + N, Lagrange interpolation results. This can be easily verified by solving directly for  $S_{\ell}$  from (39) with m = M + N. For the optimizations carried out next, the imposed order will be less than M + N, which frees up some of the coefficients  $a_n^{(\ell)}$  for optimization.

The second condition is to ensure that for the point that falls on the grid,  $t' = t_j$ , the interpolation will return exactly the value at the grid point, i.e., by (19), we require that

$$p(t_j) = \sum_{\ell=-M}^{N} S_{\ell}(0)u^{j+\ell} = u^j$$
(41)

This leads to

CONSTRAINT II: 
$$a_0^{(0)} = 1$$
, and  $a_0^{(\ell)} = 0$ ,  $\ell \neq 0$  (42)

#### A. Optimized one-sided temporal basis functions.

We first present the optimized temporal basis functions where the interpolation stencil is one-sided. As an example, for the case of M=3 and N=0, while the maximum possible order for the basis functions is 3, the imposed order is a reduced one at m=1. After carrying out the minimization of (38), subject to the constraints given in (40) and (42), the optimized basis function is as follows:

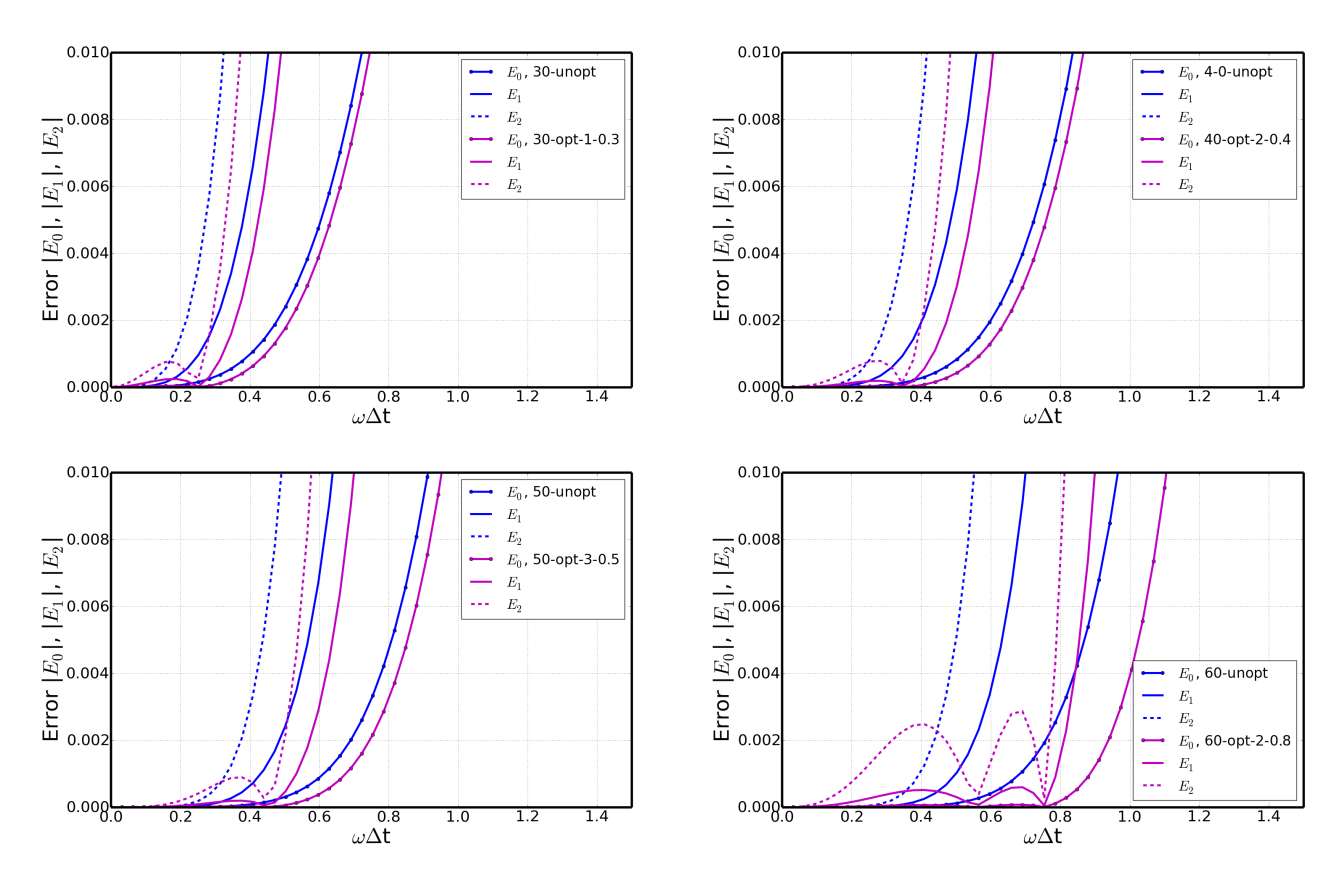


Figure 6. Interpolation errors of optimized one-sided temporal basis functions.

$$\bar{\Psi}(\tau) = \begin{cases}
1 + 1.8201575\tau + 0.97676292\tau^2 + 0.15665311\tau^3 & -1 < \tau \le 0 \\
1.0001132 + 0.49560144\tau - 1.0150542\tau^2 - 0.48066045\tau^3 & 0 < \tau \le 1 \\
1.0192289 - 0.54628682\tau - 0.96438694\tau^2 + 0.49136155\tau^3 & 1 < \tau \le 2 \\
0.99549608 - 1.8336787\tau + 1.0026782\tau^2 - 0.16735421\tau^3 & 2 < \tau \le 3 \\
0 & \text{other}
\end{cases}$$
(43)

Compared to the un-optimized one shown in (14), we see that the coefficients now get slightly modified. For this particular optimization, the value of  $\xi_0$  in (38) has been taken to be 0.3. The optimized basis function will be denoted as **30-opt-1-0.3**, following the schematic notation of "MN-opt-m- $\xi_0$ ", indicating that the temporal basis function uses a stencil from  $t_{j-M}$  to  $t_{j+N}$  with an optimization of imposed order m and a limit  $\xi_0$  in the objective integral (38). Here,  $\xi_0$  is an adjustable parameter that defines the range of non-dimensional frequency  $\omega \Delta t$  for optimization. The value of  $\xi_0$  can be made larger or smaller depending on the maximum tolerable error for interpolation.

The interpolation errors in the Fourier space of the optimized and un-optimized basis functions are shown and compared in Figure 6, for one-sided stencils with  $M=3,\,4,\,5$  and 6. The coefficients of the optimized basis functions are given in Appendix B, tables 4-9. In each of the cases, it is seen that the resolution of optimized interpolation has been extended to higher frequencies compared to the un-optimized ones. It is also seen that, due to the reduced formal order of interpolation, the error at lower frequencies is somewhat elevated. However, the increased error is kept at a practically insignificant levels and is controllable by varying  $\xi_0$ . For the special case of M=6 and N=0, it is noted that the un-optimized as well as as optimized schemes at an order higher than 2 are found to be unstable. The particular optimized scheme **60-opt-2-0.8** shown in Figure 6 are stable in the numerical tests conducted in the current study.

#### B. Two-sided

Optimization for interpolations using two-sided stencils has also been performed. The errors for the various two-sided schemes are shown in Figure 7. The gain in resolution by the optimization is more significant for wider stencils. For instance, for the M4N3 schemes, using a criteria of  $|E_2| \leq 0.001$ , the accuracy limit is increased from  $\omega \Delta t \leq 0.7$  to  $\omega \Delta t \leq 0.9$ , an increase of 28% in resolution.

The coefficients of the optimized two-sided basis functions for selected stencils are given in Appendix B, Tables 10-12.

## V. Applications of optimized temporal basis functions

In this section, the optimized temporal basis functions are applied to the numerical solution for scattering of a point source by a sphere, as shown in Figure 8. The sphere is assumed to have a rigid surface for which an analytical solution exists. The radius of the sphere is 0.5 and a point source is placed at  $\mathbf{r} = (0,0,1)$ . By solving the time domain boundary integral equation, scattering solutions at all frequencies, within the resolution of time domain temporal basis functions used, are computed in one single time domain calculation.

To examine the accuracy and benefits of the optimized temporal basis functions, the solution along a line in the plane z = -2.5 will be computed and compared with the exact solution, as shown in Figure 8. For the examples presented in this section, 32,642 constant elements are used. Here, the extra fine resolution in space is used for the purpose of isolating as much as possible the errors by the temporal basis functions from that by the spatial discretization. Further details on the numerical procedures are referred to [19].

#### A. Optimized one-sided temporal basis functions

We first show the results of optimized one-sided temporal basis functions and the comparisons with that of the un-optimized shifted Lagrange basis functions. In Figure 9, the converted frequency domain solution as a

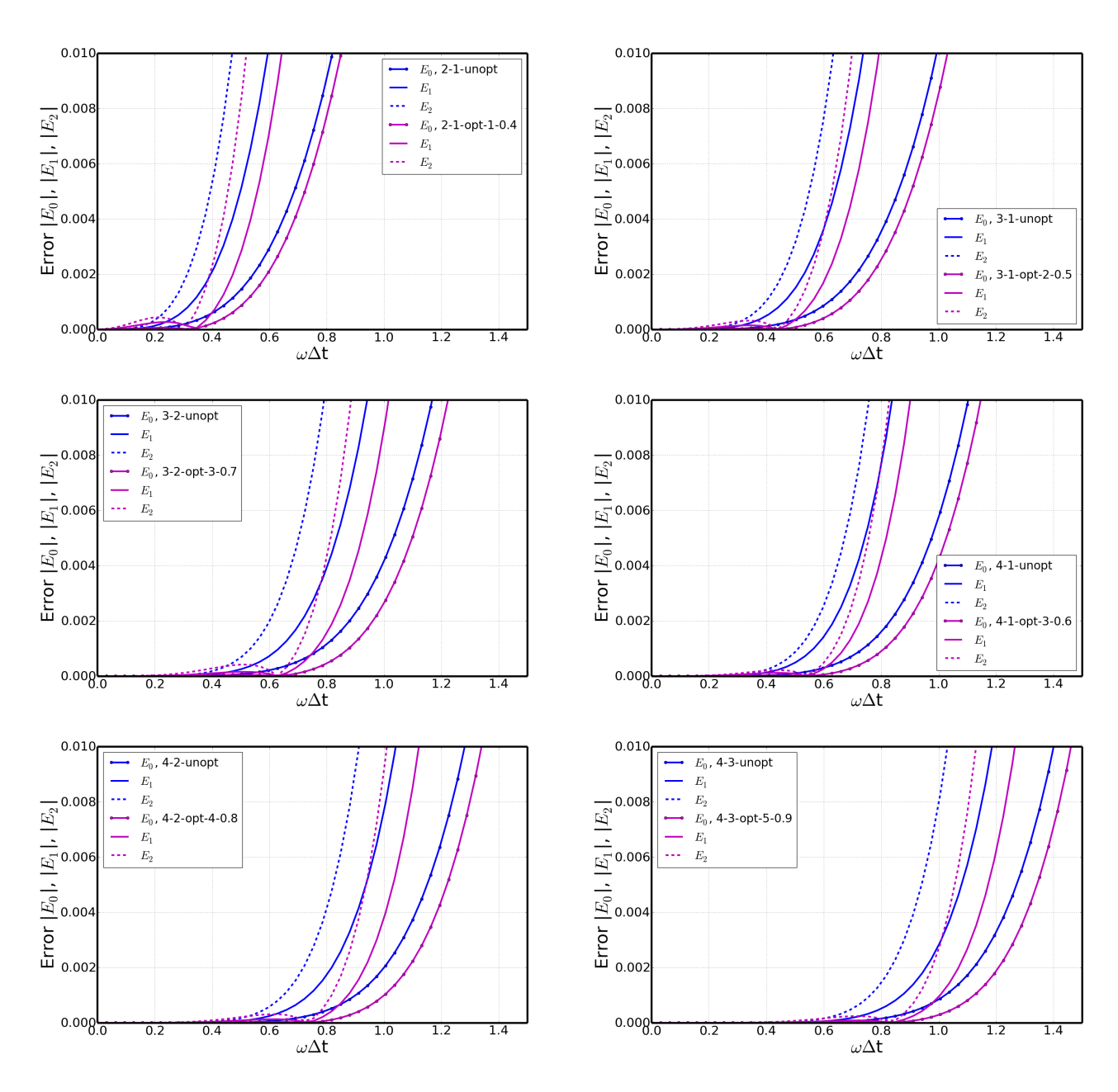


Figure 7. Errors of optimized two-sides temporal basis functions.

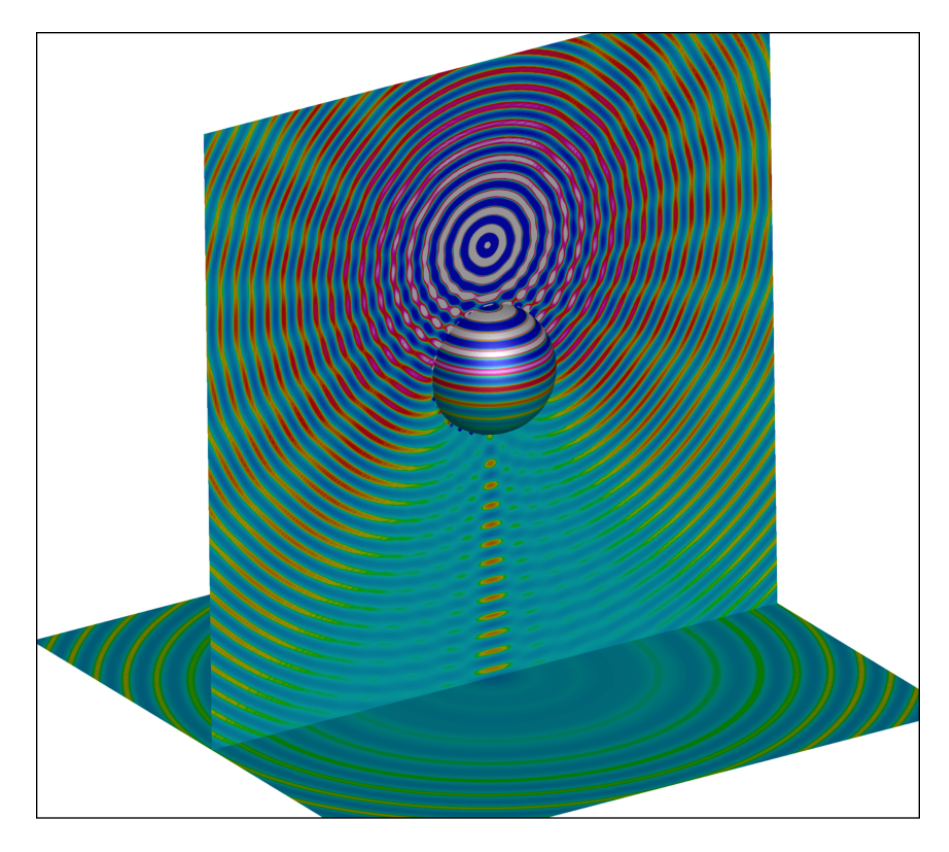


Figure 8. Converted frequency domain solution, scattering of a point source by a sphere.

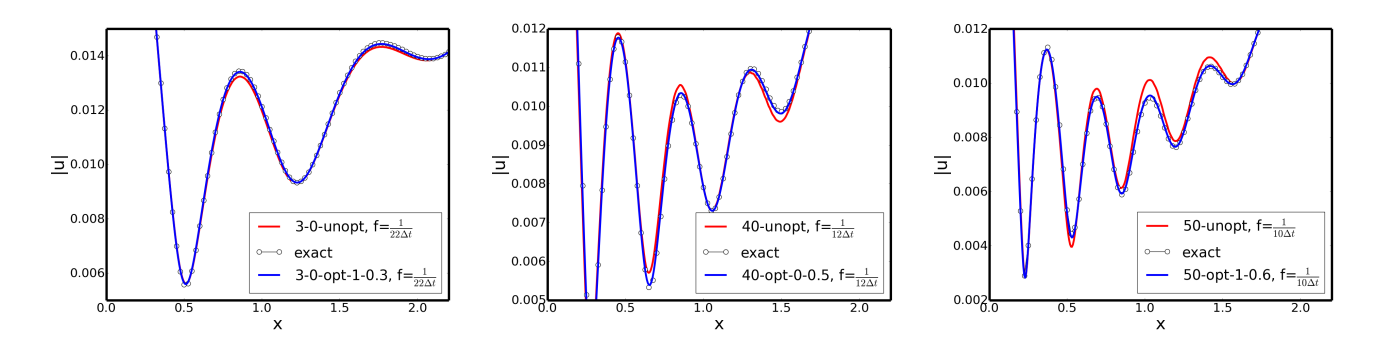


Figure 9. Scattering solutions by un-optimized and optimized temporal basis functions.

function of x along the line y=0, z=-2.5 are plotted. For each case, the solutions by the un-optimized and optimized basis functions at a chosen frequency are shown, to demonstrate the benefits of the optimized ones. The chosen frequency is such that the solution by the optimized basis functions is still accurate while that by the un-optimized basis functions is showing larger errors. This indicates that the use of optimized basis functions provides more accurate solutions when the same time step size has been used. As the optimization for basis functions results in simply a different set of coefficients for the temporal basis polynomials, there should be no additional computational cost incurred compared to the un-optimized ones.

To demonstrate further the quantitative behavior of the numerical error, a relative error in the L2 norm is computed for each case:

$$E_{L2} = \frac{||\hat{u} - \hat{u}_e||_2}{||\hat{u}||_2} \tag{44}$$

where  $\hat{u}$  and  $\hat{u}_e$  are the numerical and exact frequency domain solutions respectively.

In Figure 10, the relative error  $E_{L2}$  is plotted as a function of the frequency for various optimized and un-optimized temporal basis functions. In all the computations in Figure 10, the time step has been kept the same with  $\Delta t = 0.0125$ . It is seen that the use of optimized basis functions keeps the error low for a larger range in the frequency space. Conversely, for a given range of frequency of interest, a larger time step can used with the optimized temporal basis functions to achieve an acceptable accuracy, resulting in a significant increase in computational efficiency and, at the same time, reduction in memory requirement.

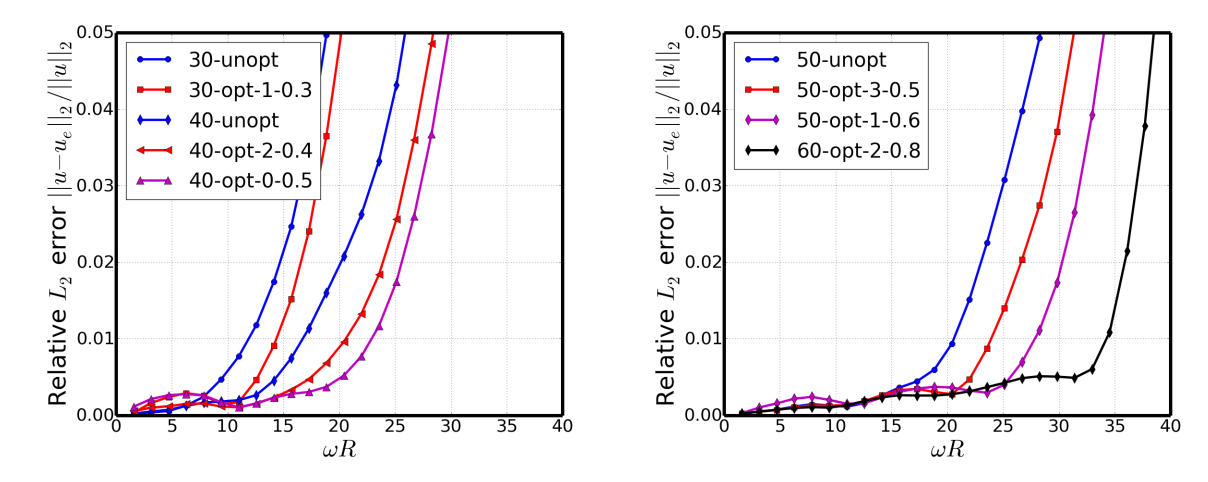


Figure 10. Relative  $L_2$  errors as a function of the frequency. All computations are made with  $\Delta t = 0.0125$ . Benefits of using optimized temporal basis functions are shown with more accurate solutions at a higher frequency compared to that using un-optimized ones.

#### B. Hybrid temporal basis functions

As noted in Section 2, when the retarded time that is a few time steps earlier than the current time, specifically when the condition (36) is satisfied, two-sided interpolation can and should be employed. Here, we present the results by a mixed use of one-sided and two-sided basis functions. When the retarded time  $t_R'$  falls within the interval  $(t_{n-1}, t_n)$  that is immediately after the current time  $t_n$ , the one-sided basis functions (N = 0) are used; otherwise, the two-sided basis functions  $(N \ge 1)$  are applied as indicated. Figure 11 shows the relative errors in L2 norms where hybrid basis functions are used, as a function of the frequency while keeping the time step size  $\Delta t = 0.0125$  in all the cases. As can be seen, in general, using the two-sided basis functions improves the accuracy. However, the improvements are not as significant as those in Figure 10 between the optimized and un-optimized basis functions. This is mainly because the accuracy of the solution is now limited by the basis functions used for the most current interval  $(t_{n-1}, t_n)$ , which has a lower

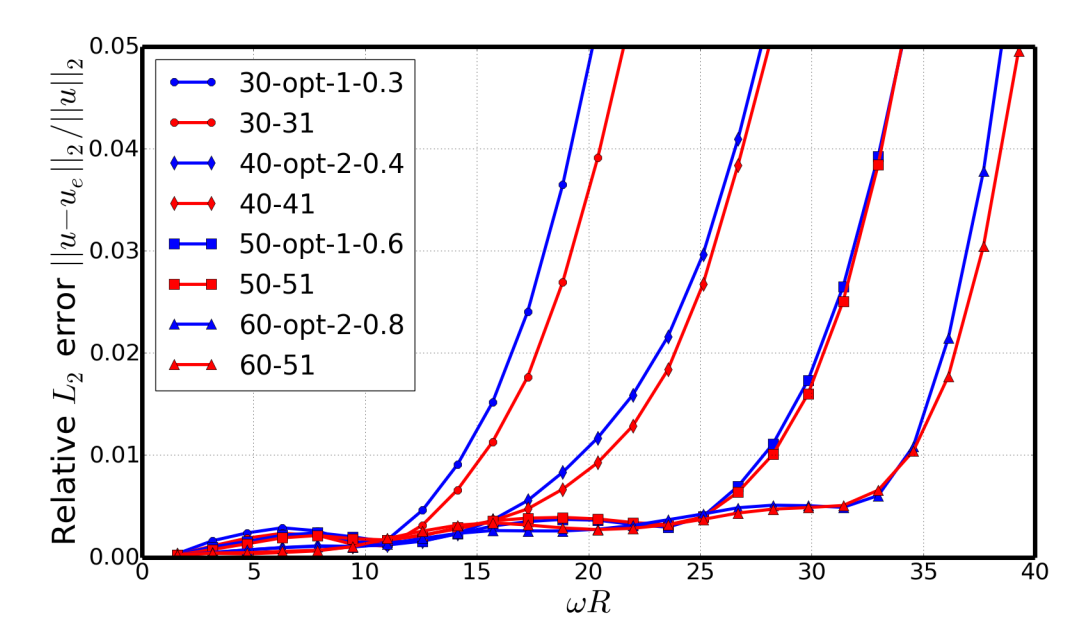


Figure 11. Relative error in L2 norm for mixed basis functions. For the results shown in blue curves, one-sided A one-sided basis functions are used for the most current time interval and a two-sided basis function is used for the rest of the intervals. Results by the one-sided and two-sided hybrid basis functions are shown in red curves. The stencils of the schemes are as indicated.

resolution compared to the two-sided one used in the rest of the time intervals. To fully take advantages of two-sided basis functions, further improvements for interpolations in the most current interval will be required.

# VI. Scattering of a point source by a flat plate and comparison with experimental results

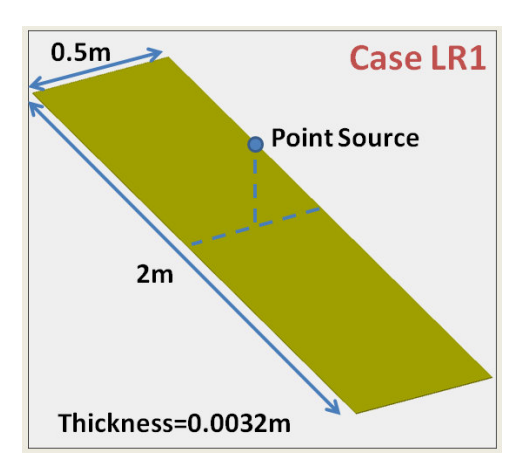
In this section, we present an application of the time domain integral equation solver to the scattering of a point source by a flat plate. An experimental study had been conducted in the early 80s of such a problem in connection with the investigation for the noise shielding effects by an aircraft body.<sup>1</sup> The computational solution will be compared with the experimental results given in [1].

The dimension of the plate is  $2m \times 0.5m \times 0.0032m$ , as shown in Figure 12. To cover the range of frequency in the experiment, up to 20kHz, a mesh of 801x 201 elements is used on the top and bottom surfaces of the plate. Along the thickness of the plate, 4 elements are used. This leads to a total of 330,018 constant elements for the discretization of the plate surface.

In the first case of the experiment, denoted as Case LR1, a point source is placed 0.25 meters above the center of the plate, as shown in Figure 12 (left). The scattered sound below the plate along a microphones traverse line is measured in the experiments, see Figure 12 (right). In the coordinate setup shown in Figure 12, the top surface of the plate is located at z=0 and the microphone traverse line is located on the plane z=-2.5 (meters) and along the line y=0. To assess the sound shielding effects, measurements of sound pressure with and without the plate are made. The shielding of sound is calculated as

$$\Delta SPL = 20 \log \left( \frac{|p_s|}{|p_u|} \right) \tag{45}$$

where  $p_s$  and  $p_u$  are the shielded and un-shielded sound pressures, respectively.<sup>1</sup>



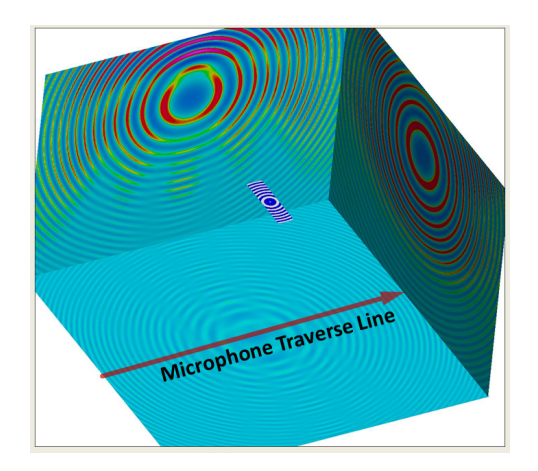


Figure 12. Left: configuration of the plate and point source in the experiment for case LR1; the dimension is in meters. Right: computational setup, which consists of the scattering body and the field points. The numerical solutions along the indicated microphone traverse line are compared with those from the experiment.

In the computation shown in Figure 12, in addition to the boundary elements on the surface of the plate for the purpose of solving the time domain boundary integral equation (1), field points are also included where the scattered sound field is computed, simulating an experimental environment, as illustrated in Figure 12(right). The point source is modeled in time by a short pulse with a broad spectrum. After the completion of the time domain simulation of (1), the frequency domain solution of all frequencies up to 20kHz becomes available at once. The converted frequency domain solution, at 3 kHz, is shown in Figure 12. More details on the numerical method can be found in [19].

Comparison with experimental results for the case LR1 is shown in Figure 13. The shielding effect, defined in (45), as a function of the traverse angle  $\theta$  is plotted at four selected frequencies of 1kHz, 4kHz, 8kHz, 12kHz, 16kHz and 20kHz. The experimental measurements are in solid black lines and the computations are in solid purple lines. The dashed lines were from the prediction given in based on a simplified edge diffraction calculation. Relatively good agreements are found between the computed and measured values on the level of shielding as well as its variation in  $\theta$ . It is to be emphasized that all the current computational results for frequency up to 20 kHz are from one single time domain calculation. <sup>19</sup>

Comparison with the experimental results for the case of LR4 is shown in Figure 14, where the location of the point source is moved to the back of the plate and is directly above one of the edges of the plate. The shielding effects at frequencies 2kHz, 8kHz, 12kHz, 16kHz and 20 kHz are plotted for both the experimental and computational results. Again, good agreements are observed on the level of shielding and its variation in  $\theta$ . Here, the traverse angle  $\theta$  is measured from the location of the point source.

#### VII. Conclusions

A Fourier analysis of the temporal basis functions used in the March-On-in-Time schemes is presented. One of the advantages of a Fourier analysis is that it provides a quantitative measure of the temporal interpolation errors in the frequency space. Temporal resolution of various well-known shifted Lagrange basis functions are presented. Based on the formulation of the Fourier analysis, optimized temporal basis functions that significantly extend the resolution in the frequency space are proposed. The optimized coefficients for the basis polynomials are given in the present paper. The substantial gain in accuracy as well as stability of the new basis functions are demonstrated by numerical examples. For instances, the accuracy limits of the conventional third-, fourth- and fifth-order shifted Lagrange basis functions are increased from 25, 18 and 14 points per wave period to 22, 12 and 10 points per wave period by using the optimized temporal basis functions respectively. The use of optimized basis functions keeps the error low for a larger range in the frequency space, and for a given range of frequency of interest, a larger time step can used with

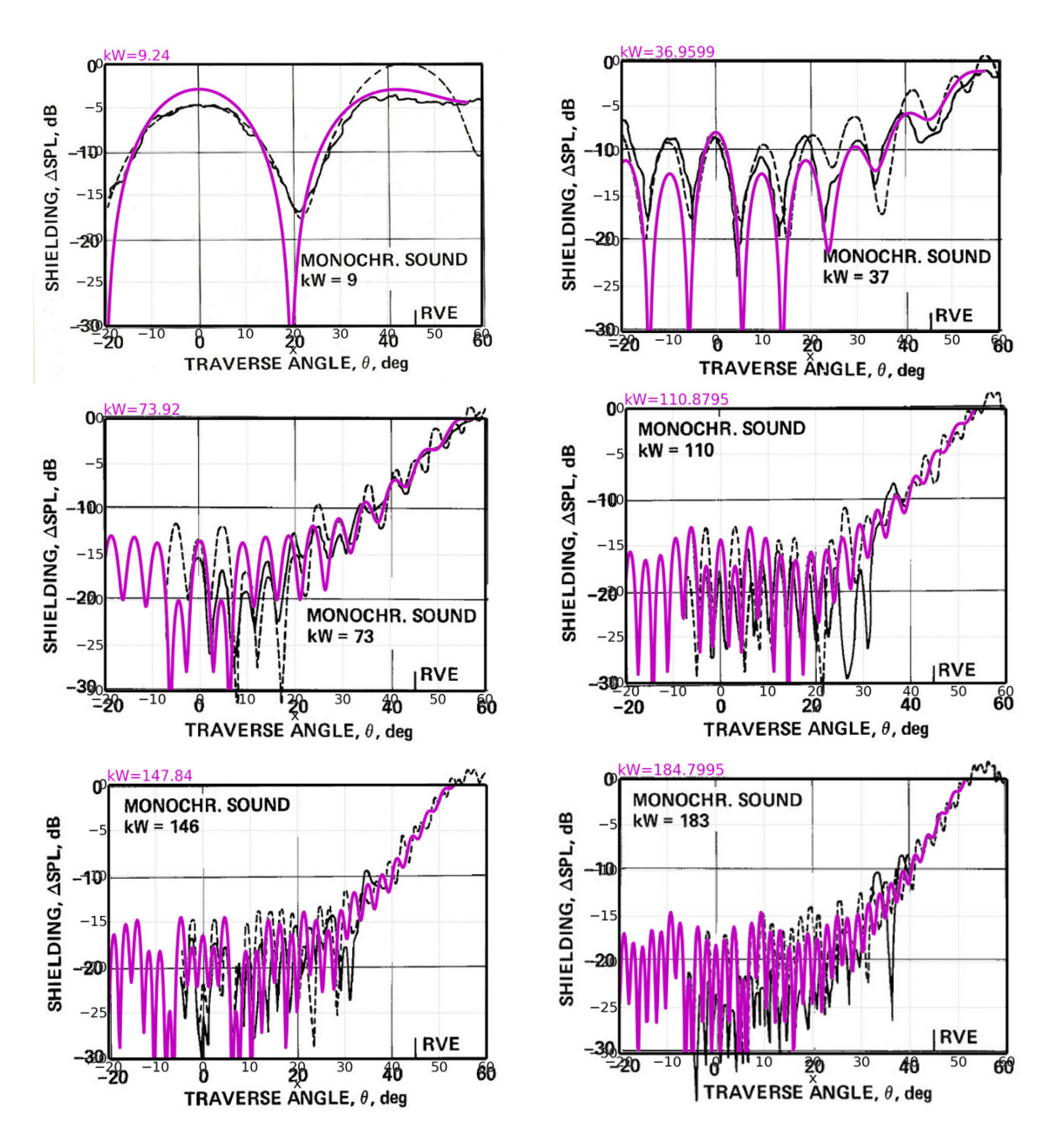


Figure 13. Case LR1. Comparison of computational and experimental results, at frequencies 1kHz, 4kHz, 8kHz, 12kHz, 16kHz and 20Hz as indicated. Black: experimental measurements; purple: current computation.

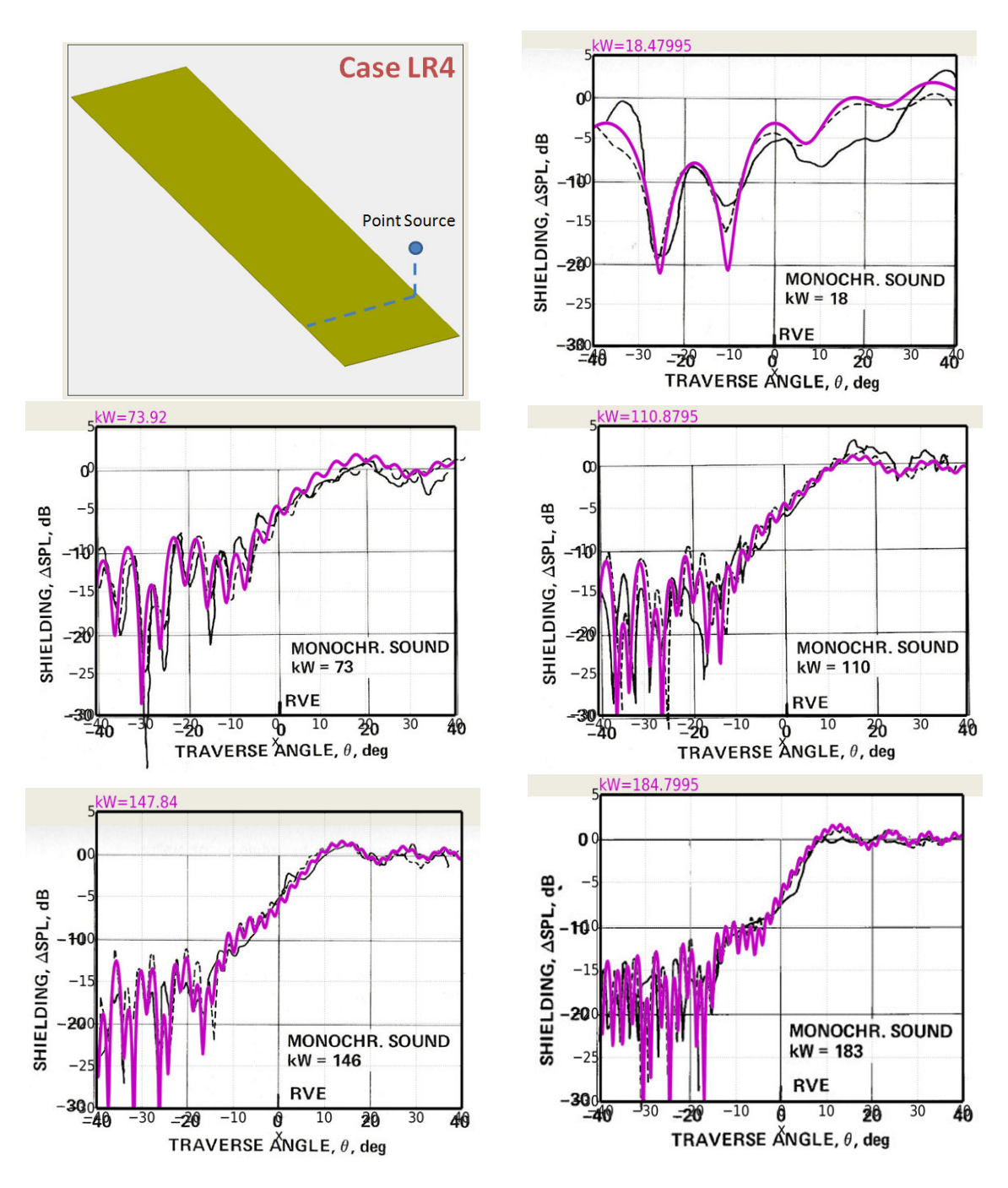


Figure 14. Case LR4. Comparison of computational and experimental results, at frequencies 2kHz, 8kHz, 12kHz, 16kHz and 20Hz as indicated. Black: experimental measurements; purple: current computation.

the optimized temporal basis functions. The increased time step size not only results in an increase in computational efficiency, it reduces substantially the requirement on the memory as well.

Moreover optimization for both one-sided and two-sided basis functions has been carried out. While significant gains in accuracy are observed for the optimized one-sided basis functions, the improvements by further using the two-sided basis functions are not as substantial. This indicates that the overall accuracy is limited by the interpolation scheme used for the most current interval.

In addition, numerical results for the scattering of a point source by a flat plate are also presented and compared with experimental measurements. The full configuration of the experiment are modeled and all the frequencies covered in the experiments are included in one single time domain simulation. Very good agreements are observed.

## Acknowledgments

This work is supported by a NASA Cooperative Agreement, NNX11AI63A. Technical monitor is Dr. Douglas M. Nark. This work used the Extreme Science and Engineering Discovery Environment (XSEDE), which is supported by National Science Foundation grant number OCI-1053575.

#### APPENDIX A.

Two-sided shifted Lagrange basis functions are given, as  $\tau$ -normalized basis functions  $\bar{\Psi}_{\ell}(\tau)$ , in Tables 1, 2 and 3.

	M=2, N=1	M = 3, N = 1	M=3, N=2
$ar{\Psi}_2$			$1 + \frac{137}{60}\tau + \frac{15}{8}\tau^2 + \frac{17}{24}\tau^3 + \frac{1}{8}\tau^4 + \frac{1}{120}\tau^5$
$ar{\Psi}_1$	$1 + \frac{11}{6}\tau + \tau^2 + \frac{1}{6}\tau^3$	$1 + \frac{25}{12}\tau + \frac{35}{24}\tau^2 + \frac{5}{12}\tau^3 + \frac{1}{24}\tau^4$	$1 + \frac{13}{12}\tau - \frac{5}{8}\tau^2 - \frac{25}{24}\tau^3 - \frac{3}{8}\tau^4 - \frac{1}{24}\tau^5$
$ar{\Psi}_0$	$1 + \frac{1}{2}\tau - \tau^2 - \frac{1}{2}\tau^3$	$1 + \frac{5}{6}\tau - \frac{5}{6}\tau^2 - \frac{5}{6}\tau^3 - \frac{1}{6}\tau^4$	$1 + \frac{1}{3}\tau - \frac{5}{4}\tau^2 - \frac{5}{12}\tau^3 + \frac{1}{4}\tau^4 + \frac{1}{12}\tau^5$
$ar{\Psi}_{-1}$	$1 - \frac{1}{2}\tau - \tau^2 + \frac{1}{2}\tau^3$	$1 - \frac{5}{4}\tau^2 + \frac{1}{4}\tau^4$	$1 - \frac{1}{3}\tau - \frac{5}{4}\tau^2 + \frac{5}{12}\tau^3 + \frac{1}{4}\tau^4 - \frac{1}{12}\tau^5$
$ar{\Psi}_{-2}$	$1 - \frac{11}{6}\tau + \tau^2 - \frac{1}{6}\tau^3$	$1 - \frac{5}{6}\tau - \frac{5}{6}\tau^2 + \frac{5}{6}\tau^3 - \frac{1}{6}\tau^4$	$1 - \frac{13}{12}\tau - \frac{5}{8}\tau^2 + \frac{25}{24}\tau^3 - \frac{3}{8}\tau^4 + \frac{1}{24}\tau^5$
$ar{\Psi}_{-3}$		$1 - \frac{25}{12}\tau + \frac{35}{24}\tau^2 - \frac{5}{12}\tau^3 + \frac{1}{24}\tau^4$	$1 - \frac{137}{60}\tau + \frac{15}{8}\tau^2 - \frac{17}{24}\tau^3 + \frac{1}{8}\tau^4 - \frac{1}{120}\tau^5$

Table 1. Two-sided shifted Lagrange basis functions M2N1, M3N1 and M3N2 schemes.

#### APPENDIX B.

Optimized one-sided basis functions are given in this appendix. The optimized schemes are denote as **MN-opt-m-** $\xi_0$  for a stencil from  $t_{j-M}$  to  $t_{j+N}$  of order m and a value of  $\xi_0$  used in the optimization of (38).

	M=4, N=1	M=4, N=2
$ar{\Psi}_2$		$1 + \frac{49}{20}\tau + \frac{203}{90}\tau^2 + \frac{49}{48}\tau^3 + \frac{35}{144}\tau^4 + \frac{7}{240}\tau^5 + \frac{1}{720}\tau^6$
$ar{\Psi}_1$	$1 + \frac{137}{60}\tau + \frac{15}{8}\tau^2 + \frac{17}{24}\tau^3 + \frac{1}{8}\tau^4 + \frac{1}{120}\tau^5$	$1 + \frac{77}{60}\tau - \frac{49}{120}\tau^2 - \frac{7}{6}\tau^3 - \frac{7}{12}\tau^4 - \frac{7}{60}\tau^5 - \frac{1}{120}\tau^6$
$ar{\Psi}_0$	$1 + \frac{13}{12}\tau - \frac{5}{8}\tau^2 - \frac{25}{24}\tau^3 - \frac{3}{8}\tau^4 - \frac{1}{24}\tau^5$	$1 + \frac{7}{12}\tau - \frac{7}{6}\tau^2 - \frac{35}{48}\tau^3 + \frac{7}{48}\tau^4 + \frac{7}{48}\tau^5 + \frac{1}{48}\tau^6$
$ar{\Psi}_{-1}$	$1 + \frac{1}{3}\tau - \frac{5}{4}\tau^2 - \frac{5}{12}\tau^3 + \frac{1}{4}\tau^4 + \frac{1}{12}\tau^5$	$1 - \frac{49}{36}\tau^2 + \frac{7}{18}\tau^4 - \frac{1}{36}\tau^6$
$ar{\Psi}_{-2}$	$1 - \frac{1}{3}\tau - \frac{5}{4}\tau^2 + \frac{5}{12}\tau^3 + \frac{1}{4}\tau^4 - \frac{1}{12}\tau^5$	$1 - \frac{7}{12}\tau - \frac{7}{6}\tau^2 + \frac{35}{48}\tau^3 + \frac{7}{48}\tau^4 - \frac{7}{48}\tau^5 + \frac{1}{48}\tau^6$
$\bar{\Psi}_{-3}$	$1 - \frac{13}{12}\tau - \frac{5}{8}\tau^2 + \frac{25}{24}\tau^3 - \frac{3}{8}\tau^4 + \frac{1}{24}\tau^5$	$1 - \frac{77}{60}\tau - \frac{49}{120}\tau^2 + \frac{7}{6}\tau^3 - \frac{7}{12}\tau^4 + \frac{7}{60}\tau^5 - \frac{1}{120}\tau^6$
$ar{\Psi}_4$	$1 - \frac{137}{60}\tau + \frac{15}{8}\tau^2 - \frac{17}{24}\tau^3 + \frac{1}{8}\tau^4 - \frac{1}{120}\tau^5$	$1 - \frac{49}{20}\tau + \frac{203}{90}\tau^2 - \frac{49}{48}\tau^3 + \frac{35}{144}\tau^4 - \frac{7}{240}\tau^5 + \frac{1}{720}\tau^6$

Table 2. Two-sided shifted Lagrange basis functions M4N1 and M4N2 schemes.

	M=4, N=3
$ar{\Psi}_3$	$1 + \frac{363}{140}\tau + \frac{469}{180}\tau^2 + \frac{967}{720}\tau^3 + \frac{7}{18}\tau^4 + \frac{23}{360}\tau^5 + \frac{1}{180}\tau^6 + \frac{1}{5040}\tau^7$
$ar{\Psi}_2$	$1 + \frac{29}{20}\tau - \frac{7}{36}\tau^2 - \frac{889}{720}\tau^3 - \frac{7}{9}\tau^4 - \frac{77}{360}\tau^5 - \frac{1}{36}\tau^6 - \frac{1}{720}\tau^7$
$ar{\Psi}_1$	$1 + \frac{47}{60}\tau - \frac{21}{20}\tau^2 - \frac{77}{80}\tau^3 + \frac{7}{40}\tau^5 + \frac{1}{20}\tau^6 + \frac{1}{240}\tau^7$
$ar{\Psi}_0$	$1 + \frac{1}{4}\tau - \frac{49}{36}\tau^2 - \frac{49}{144}\tau^3 + \frac{7}{18}\tau^4 + \frac{7}{72}\tau^5 - \frac{1}{36}\tau^6 - \frac{1}{144}\tau^7$
$ar{\Psi}_{-1}$	$1 - \frac{1}{4}\tau - \frac{49}{36}\tau^2 + \frac{49}{144}\tau^3 + \frac{7}{18}\tau^4 - \frac{7}{72}\tau^5 - \frac{1}{36}\tau^6 + \frac{1}{144}\tau^7$
$ar{\Psi}_{-2}$	$1 - \frac{47}{60}\tau - \frac{21}{20}\tau^2 + \frac{77}{80}\tau^3 - \frac{7}{40}\tau^5 + \frac{1}{20}\tau^6 - \frac{1}{240}\tau^7$
$\bar{\Psi}_{-3}$	$1 - \frac{29}{20}\tau - \frac{7}{36}\tau^2 + \frac{889}{720}\tau^3 - \frac{7}{9}\tau^4 + \frac{77}{360}\tau^5 - \frac{1}{36}\tau^6 + \frac{1}{720}\tau^7$
$ar{\Psi}_4$	$1 - \frac{363}{140}\tau + \frac{469}{180}\tau^2 - \frac{967}{720}\tau^3 + \frac{7}{18}\tau^4 - \frac{23}{360}\tau^5 + \frac{1}{180}\tau^6 - \frac{1}{5040}\tau^7$

Table 3. Two-sided shifted Lagrange basis functions for the M4N3 scheme.

For convenience of implementation, the optimized basis functions are given both as  $S_{\ell}(\eta)$  in (20) and as the  $\tau$ -normalized basis function  $\bar{\Psi}_{\ell}(\tau)$ ,  $\ell = -M, ..., N$ , where

$$S_{\ell}(\eta) = \sum_{n=0}^{M+N} a_n^{(\ell)} \eta^n$$

$$\bar{\Psi}_\ell(\tau) = \sum_{n=0}^{M+N} b_n^{(\ell)} \tau^n$$

The optimized coefficients for one-sided schemes are listed in tables 4-9, and for two-sided schemes are listed in tables 10-12.

30-opt-1-0.3:		
$a_0^{(0)} = 1, \ a_1^{(0)} = -1.820157538622123, \ a_2^{(0)} = 0.9767629249288535, \ a_3^{(0)} = -0.1566531198507175$		
$a_0^{(-1)} = 0, \ a_1^{(-1)} = 2.976488345219672, \ a_2^{(-1)} = -2.457035584498764, \ a_3^{(-1)} = 0.4806604580295282$		
$a_0^{(-2)} = 0, \ a_1^{(-2)} = -1.492504074572975, \ a_2^{(-2)} = 1.983782394210968, \ a_3^{(-2)} = -0.4913615565069039$		
$a_0^{(-3)} = 0, \ a_1^{(-3)} = 0.3361732679754260, \ a_2^{(-3)} = -0.5035097346410570, \ a_3^{(-3)} = 0.1673542183280932$		
$b_0^{(0)} = 1, \ b_1^{(0)} = 1.820157538622123, \ b_2^{(0)} = 0.9767629249288535, \ b_3^{(0)} = 0.1566531198507175$		
$b_0^{(-1)} = 1.000113218750436, \ b_1^{(-1)} = 0.4956014496892710, \ b_2^{(-1)} = -1.015054210410179, \ b_3^{(-1)} = -0.4806604580295282$		
$b_0^{(-2)} = 1.019228975642691, \ b_1^{(-2)} = -0.5462868241880500, \ b_2^{(-2)} = -0.9643869448304550, \ b_3^{(-2)} = 0.4913615565069039$		
$b_0^{(-3)} = 0.9954960870152810, \ b_1^{(-3)} = -1.833678754987600, \ b_2^{(-3)} = 1.002678230311782, \ b_3^{(-3)} = -0.1673542183280932$		

Table 4. Optimized coefficients of a one-sided scheme 30-opt-1-0.3 for M=3 and N=0.

40-opt-2-0.4:
$a_0^{(0)} = 1, \ a_1^{(0)} = -2.062150691362142, \ a_2^{(0)} = 1.411138926293613, \ a_3^{(0)} = -0.3815749670613513, \ a_4^{(0)} = 0.03258852451576015$
$a_0^{(-1)} = 0, \ a_1^{(-1)} = 3.940193508706198, \ a_2^{(-1)} = -4.195717425454449, \ a_3^{(-1)} = 1.393477742162557, \ a_4^{(-1)} = -0.1379601918306038$
$a_0^{(-2)} = 0, \ a_1^{(-2)} = -2.947676377945740, \ a_2^{(-2)} = 4.620318718601672, \ a_3^{(-2)} = -1.890983424119563, \ a_4^{(-2)} = 0.2183494283972505$
$a_0^{(-3)} = 0, \ a_1^{(-3)} = 1.323374995221450, \ a_2^{(-3)} = -2.298040866014450, \ a_3^{(-3)} = 1.127833489996861, \ a_4^{(-3)} = -0.1531723793657302$
$a_0^{(-4)} = 0, \ a_1^{(-4)} = -0.253741434619772, \ a_2^{(-4)} = 0.46230064657361, \ a_3^{(-4)} = -0.248752840978503, \ a_4^{(-4)} = 0.04019461828332335$
$b_0^{(0)} = 1, \ b_1^{(0)} = 2.062150691362142, \ b_2^{(0)} = 1.411138926293613, \ b_3^{(0)} = 0.3815749670613513,$
$b_4^{(0)} = 0.03258852451576015$
$b_0^{(-1)} = 0.9999936335837022, \ b_1^{(-1)} = 0.8226488830374440, \ b_2^{(-1)} = -0.8430453499504010, \ b_3^{(-1)} = -0.8416369748401418,$
$b_4^{(-1)} = -0.1379601918306038$
$b_0^{(-2)} = 0.9516455799147180, \ b_1^{(-2)} = 0.1710208842617900, \ b_2^{(-2)} = -1.485195544581696, \ b_3^{(-2)} = 0.1441879969415590,$
$b_4^{(-2)} = 0.2183494283972505$
$b_0^{(-3)} = 1.332298692825400, \ b_1^{(-3)} = -1.444017057551140, \ b_2^{(-3)} = -0.4188479417921300, \ b_3^{(-3)} = 0.7102350623919010,$
$b_4^{(-3)} = -0.1531723793657302$
$b_0^{(-4)} = 0.7514850646052620, \ b_1^{(-4)} = -1.794349651531750, \ b_2^{(-4)} = 1.335949910030616, \ b_3^{(-4)} = -0.3943610515546706,$
$b_4^{(-4)} = 0.04019461828332335$

Table 5. Optimized coefficients of a one-sided scheme 40-opt-2-0.4 for M=4 and N=0.

## 40-opt-0-0.5: $a_0^{(0)} = 1, \ a_1^{(0)} = -2.034105581242223, \ a_2^{(0)} = 1.348564342790794, \ a_3^{(0)} = -0.3349900179133711, \ a_4^{(0)} = 0.02053535385764966$ $a_0^{(-1)} = 0, \ a_1^{(-1)} = 3.861902518822506, \ a_2^{(-1)} = -4.015123947967559, \ a_3^{(-1)} = 1.253368113587240, \ a_4^{(-1)} = -0.1001612149114932$ $a_0^{(-2)} = 0, \ a_1^{(-2)} = -2.875187020819725, \ a_2^{(-2)} = 4.441354241058630, \ a_3^{(-2)} = -1.741242953899078, \ a_4^{(-2)} = 0.1750950769588371$ $a_0^{(-3)} = 0, \ a_1^{(-3)} = 1.304038639460538, \ a_2^{(-3)} = -2.237608224395451, \ a_3^{(-3)} = 1.066275342579155, \ a_4^{(-3)} = -0.1327171661167696$ $a_0^{(-4)} = 0, \ a_1^{(-4)} = -0.256648556221096, \ a_2^{(-4)} = 0.462813588513586, \ a_3^{(-4)} = -0.243410484353946, \ a_4^{(-4)} = 0.037247950211776$ $b_0^{(0)} = 1, b_1^{(0)} = 2.034105581242223, b_2^{(0)} = 1.348564342790794, b_3^{(0)} = 0.3349900179133711,$ $b_4^{(0)} = 0.02053535385764966$ $b_0^{(-1)} = 0.9999854695306938, \ b_1^{(-1)} = 0.8088858959968650, \ b_2^{(-1)} = -0.8559868966747980, \ b_3^{(-1)} = -0.8527232539412672,$ $b_4^{(-1)} = -0.1001612149114932$ $b_0^{(-2)} = 0.8866205227438440, \ b_1^{(-2)} = 0.4016430406913600, \ b_2^{(-2)} = -1.803821635323750, \ b_3^{(-2)} = 0.3404823382283810,$ $b_4^{(-2)} = 0.1750950769588371$ $b_4^{(-3)} = -0.1327171661167696$ $b_4^{(-4)} = 0.03724795021177600$

Table 6. Optimized coefficients of a one-sided scheme 40-opt-0-0.5 for M=4 and N=0.

```
50-opt-3-0.5:
                                                   a_0^{(0)} = 1, \ a_1^{(0)} = -2.253708396282178, \ a_2^{(0)} = 1.802980567846060, \ a_3^{(0)} = -0.6435629579203238,
                                                                                                                   a_4^{(0)} = 0.09800825706055226, \ a_5^{(0)} = -0.003717475566444615
                                            a_0^{(-1)} = 0, \ a_1^{(-1)} = 4.885997199963343, \ a_2^{(-1)} = -6.133796019327818, \ a_3^{(-1)} = 2.696612864444295,
                                                                                                                        a_4^{(-1)} = -0.4705165275321261, \ a_5^{(-1)} = 0.02170250467191372
                                         a_0^{(-2)} = 0, \ a_1^{(-2)} = -4.840238170364923, \ a_2^{(-2)} = 8.505378398850670, \ a_3^{(-2)} = -4.517488545240609, \ a_3^{(-2)} = -4.517488545240609,
                                                                                                                       a_4^{(-2)} = 0.9019835395229814, \ a_5^{(-2)} = -0.04963526302320873
                                            a_0^{(-3)} = 0, \ a_1^{(-3)} = 3.241815274136500, \ a_2^{(-3)} = -6.243164759045710, \ a_3^{(-3)} = 3.808418028259290,
                                       a_4^{(-3)} = -0.8629340239817120, \ a_5^{(-3)} = 0.05586551670259000 a_0^{(-4)} = 0, \ a_1^{(-4)} = -1.238362855620700, \ a_2^{(-4)} = 2.490475559620370, \ a_3^{(-4)} = -1.633007088972323,
                                                                                                                     a_4^{(-4)} = 0.4119422542202200, \ a_5^{(-4)} = -0.0310478851909856
                                     a_0^{(-5)} = 0, \ a_1^{(-5)} = 0.2044969481679640, \ a_2^{(-5)} = -0.4218737479435780, \ a_3^{(-5)} = 0.2890276994296667,
                                                                                                                    a_4^{(-5)} = -0.07848349928991710, \ a_5^{(-5)} = 0.006832602406135260
                                                            b_0^{(0)} = 1, b_1^{(0)} = 2.253708396282178, b_2^{(0)} = 1.802980567846060, b_3^{(0)} = 0.6435629579203238,
                                                                                                                               b_4^{(0)} = 0.09800825706055226, \ b_5^{(0)} = 0.003717475566444615
      b_0^{(-1)} = 1.000000022219608, b_1^{(-1)} = 1.065309832128350, b_2^{(-1)} = -0.6500315444685530, b_3^{(-1)} = -1.031571801034928,
                                                                                                                        b_4^{(-1)} = -0.3620040041725575, \ b_5^{(-1)} = -0.02170250467191372
b_0^{(-2)} = 1.044537108372981, \ b_1^{(-2)} = 0.1359348949708500, \ b_2^{(-2)} = -0.9227689658981300, \ !b_3^{(-2)} = -0.7129692500148930, \ b_3^{(-2)} = -0.712969250014890, \ b_3^{(-2)} = -0.71296925000, \ b_3^{(-2)} = -0.71
                                                                                                                            b_4^{(-2)} = 0.4056309092908941, b_5^{(-2)} = 0.04963526302320873
      b_0^{(-3)} = 0.04191437020961000, \ b_1^{(-3)} = 1.961226842612910, \ b_2^{(-3)} = -3.482150290025250, \ b_3^{(-3)} = 1.518893756288150,
                                                                                                                  b_4^{(-3)} = -0.02495127344286200, \ b_5^{(-3)} = -0.05.586551670259000
     b_0^{(-4)} = 4.045886482021400, \ b_1^{(-4)} = -6.017025386585420, \ b_2^{(-4)} = 2.570200374862790, \ b_3^{(-4)} = 0.009592652006509000,
                                                                                                                         b_4^{(-4)} = -0.2090154495994932, b_5^{(-4)} = 0.03104788519098566
 b_0^{(-5)} = -1.096201066066790, \ b_1^{(-5)} = 0.2270301998286800, \ b_2^{(-5)} = 0.6817698576829370, \ b_3^{(-5)} = -0.4275083151651400, \ b_3^{(-5)} = 0.2270301998286800, \ b_3^{(-5)} = 0.6817698576829370, \ b_3^{(-5)} = 0.4275083151651400, \ b_3^{(-5)} = 0.427508160, \ b_3^{(-5)} = 0.4275083151651400, \ b_3^{(-5)} = 0.427508160, \ b_3^{(-5)} = 0.42750800, \ b_3^{(-5)} = 0.4275000, \ b_3^{(-5)} = 0.42750000, \ b_3^{(-5)} = 0.427500000, \ b_3^{(-5)} = 0.4275000000, \ b_3^{(-5)} = 0.4275000000000000000000000000
                                                                                                                       b_4^{(-5)} = 0.09233156086346440, \ b_5^{(-5)} = -0.006832602406135260
```

Table 7. Optimized coefficients of a one-sided scheme 50-opt-3-0.5 for M=5 and N=0.

```
\begin{array}{c} \textbf{50-opt-1-0.6:} \\ a_0^{(0)} = 1, \ a_1^{(0)} = -2.215037130002110, \ a_2^{(0)} = 1.709521692382997, \ a_3^{(0)} = -0.5603976849101513, \\ a_4^{(0)} = 0.06394402097872657, \ a_5^{(0)} = 0.001969077570047259 \\ a_0^{(-1)} = 0, \ a_1^{(-1)} = 4.742633982281605, \ a_2^{(-1)} = -5.779728449023321, \ a_3^{(-1)} = 2.371825057889128, \\ a_4^{(-1)} = -0.3324790253197149, \ a_5^{(-1)} = -0.002251452993678422 \\ a_0^{(-2)} = 0, \ a_1^{(-2)} = -4.638819984009898, \ a_2^{(-2)} = 7.989496031369253, \ a_3^{(-2)} = -4.021183642875550, \\ a_4^{(-2)} = 0.6795150419741979, \ a_5^{(-2)} = -0.009.007662381550786 \\ a_0^{(-3)} = 0, \ a_1^{(-3)} = 3.118574740431463, \ a_2^{(-3)} = -5.902228809953020, \ a_3^{(-3)} = 3.449889828358286, \\ a_4^{(-3)} = -0.6876777025009474, \ a_5^{(-3)} = 0.02144215404498828 \\ a_0^{(-4)} = 0, \ a_1^{(-4)} = -1.216039807949110, \ a_2^{(-4)} = 2.407274859976580, \ a_3^{(-4)} = -1.521540535095678, \\ a_4^{(-4)} = 0.3470062754645280, \ a_5^{(-4)} = -0.01670089682084681 \\ a_0^{(-5)} = 0, \ a_1^{(-5)} = 0.20868819924805, \ a_2^{(-5)} = -0.4243353247524800, \ a_3^{(-5)} = 0.2814069766339650, \\ a_4^{(-5)} = -0.07030861059678980, \ a_5^{(-5)} = 0.004548780581040484 \\ b_0^{(0)} = 1, \ b_1^{(0)} = 2.215037130002110, \ b_2^{(0)} = 1.709521692382997, \ b_3^{(0)} = 0.5603976849101513, \\ b_4^{(1)} = 0.06394402097872657, \ b_5^{(0)} = -0.001969077570047259 \\ b_0^{(-1)} = 1.000000112834019, \ b_1^{(-1)} = 1.0425211083449, \ b_2^{(-1)} = -0.68164195721101, \ b_3^{(-1)} = -1.019394426673484, \\ b_4^{(-1)} = -0.3437362902881070, \ b_5^{(-1)} = 0.002251452993678422 \\ b_0^{(-2)} = 1.094870489830355, \ b_1^{(-2)} = -0.8828277961078, \ b_2^{(-2)} = -0.54985780902736, \ b_3^{(-2)} = -1.054630197656002, \\ b_4^{(-2)} = 0.5894384181586900, \ b_5^{(-2)} = -0.092474215040498828 \\ b_0^{(-4)} = 8.005532456077490, \ b_1^{(-4)} = -12.46467197550624, \ b_2^{(-4)} = 6.77281691808117, \ b_3^{(-4)} = -1.35841638100128, \\ b_4^{(-4)} = 0.01298833904759180, \ b_5^{(-5)} = -0.004548780581040484 \\ b_0^{(-5)} = -4.117012350568240, \ b_1^{(-5)} = 3.
```

Table 8. Optimized coefficients of a one-sided scheme 50-opt-1-0.6 for M=5 and N=0.

```
60-opt-2-0.8:
                         \overline{a_0^{(0)}=1,\ a_1^{(0)}=-2.335338640342133,\ a_2^{(0)}=1.964165026362754,\ a_3^{(0)}=-0.7385687289262745,}
                               a_4^{(0)} = 0.1076408436734090, \ a_5^{(0)} = 0.004207072283015086, \ a_6^{(0)} = -0.002105561530452494
                      a_0^{(-1)} = 0, \ a_1^{(-1)} = 5.463663989183361, \ a_2^{(-1)} = -7.317425711495562, \ a_3^{(-1)} = 3.466208969176967,
                    a_4^{(-1)} = -0.6175063130227441, \ a_5^{(-1)} = -0.005425514102058792, \ a_6^{(-1)} = 0.01048451884945769 a_0^{(-2)} = 0, \ a_1^{(-2)} = -6.489567664533225, \ a_2^{(-2)} = 11.96384343392011, \ a_3^{(-2)} = -6.893802373593481,
                           a_4^{(-2)} = 1.467129856434025, \ a_5^{(-2)} = -0.02598815228941379, \ a_6^{(-2)} = -0.02161495904990831
                      a_0^{(-3)} = 0, \ a_1^{(-3)} = 5.720280598165229, \ a_2^{(-3)} = -1.152419880172741, \ a_3^{(-3)} = 7.569600527652864,
                              a_4^{(-3)} = -1.867044019804100, \ a_5^{(-3)} = 0.07785134875009855, \ a_6^{(-3)} = 0.02351016807234565
                    a_0^{(-4)} = 0, \ a_1^{(-4)} = -3.329996093997950, \ a_2^{(-4)} = 7.001317521175880, \ a_3^{(-4)} = -4.929546099273250,
                            a_4^{(-4)} = 1.358803395934456, \ a_5^{(-4)} = -0.08647607573845128, \ a_6^{(-4)} = -0.01410251545537654
                      a_0^{(-5)} = 0, \ a_1^{(-5)} = 1.151132947769120, \ a_2^{(-5)} = -2.483273973548600, \ a_3^{(-5)} = 1.825867637634650,
                a_{4}^{(-5)} = -0.5433076551194460, \ a_{5}^{(-5)} = 0.04523585119646552, \ a_{6}^{(-5)} = 0.004345137828776000 a_{0}^{(-6)} = 0, \ a_{1}^{(-6)} = -0.1801751362443900, \ a_{2}^{(-6)} = 0.3955725053129100, \ a_{3}^{(-6)} = -0.2997599326714800,
                      a_4^{(-6)} = 0.09428389190440000, \ a_5^{(-6)} = -0.009404530099655280, \ a_6^{(-6)} = -0.0005167887148419200
                              \overline{b_0^{(0)}=1,\ b_1^{(0)}=2.335338640342133,\ b_2^{(0)}=1.964165026362754,\ b_3^{(0)}=0.7385687289262745,}
                             b_4^{(0)} = 0.1076408436734090, \ b_5^{(0)} = -0.004.207072283015086, \ b_6^{(0)} = -0.002.105561530452494
b_0^{(-1)} = 0.999999385894208, b_1^{(-1)} = 1.206806235781379, b_2^{(-1)} = -0.5208240403798516, b_3^{(-1)} = -1.151618953054557,
                            b_4^{(-1)} = -0.4873661007911727, \ b_5^{(-1)} = -0.05748159899468735, \ b_6^{(-1)} = 0.01048451884945769
b_0^{(-2)} = 0.9849188683551670, \ b_1^{(-2)} = 0.6407913268212580, \ b_2^{(-2)} = -1.454496608355274, \ b_3^{(-2)} = -0.3453169383168390,
                            b_4^{(-2)} = -0.08964920945461200, b_5^{(-2)} = 0.2853676608883135, b_6^{(-2)} = -0.02161495904990831
   b_0^{(-3)} = 2.648491492458130, \ b_1^{(-3)} = -5.121169188855139, \ b_2^{(-3)} = 5.366547248153540, \ b_3^{(-3)} = -4.867184436579184,
   b_4^{(-3)} = 2.474598901214041, \ b_5^{(-3)} = -0.5010343740523202, \ b_6^{(-3)} = 0.02351016807234565 b_0^{(-4)} = -15.25158989284142, \ b_1^{(-4)} = 33.41923123353735, \ b_2^{(-4)} = -31.2064574816500, \ b_3^{(-4)} = 15.07608366535612,
                              b_4^{(-4)} = -3.755321828124940, \ b_5^{(-4)} = 0.4249364466674883, \ b_6^{(-4)} = -0.01410251545537654166674883, \ b_6^{(-4)} = -0.0141025166674883, \ b_6^{(-4)} = -0.0141026674883, \ b_6^{(-4)} = -0.014102674883, \ b_6^{(-4)} = -0.014102674884, \ b_6^{(-4)} = -0.01410267484, \ b_6^{(-4)} = -0.01410267484, \ b_6^{(-4)} = -0.0141026748
    b_0^{(-5)} = 41.59479921838780, \ b_1^{(-5)} = -64.4380077536637, \ b_2^{(-5)} = 40.68907346341115, \ b_3^{(-5)} = -13.13152190630211,
                                b_4^{(-5)} = 2.217015310583192, b_5^{(-5)} = -0.1755899860597455, b_6^{(-5)} = 0.00434513782877600
   b_0^{(-6)} = -26.63758250972294, \ b_1^{(-6)} = 31.39874452103854, \ b_2^{(-6)} = -14.99494326320565, \ b_3^{(-6)} = 3.655104610958875,
                           b_4^{(-6)} = -0.4669179170998952, b_5^{(-6)} = 0.02800892383396440, b_6^{(-6)} = -0.000516788714841920
```

Table 9. Optimized coefficients of a one-sided scheme 60-opt-2-0.8 for M=6 and N=0.

## 31-opt-2-0.5: $a_0^{(-1)} = 0, \ a_1^{(-1)} = 1.489665456041122, \ a_2^{(-1)} = 0.2718610147390500, \ a_3^{(-1)} = -1.012698488748735, \ a_4^{(-1)} = 0.2511765911393588122, \ a_3^{(-1)} = 0.2718610147390500, \ a_3^{(-1)} = 0.27186101473905$ $a_0^{(-2)} = 0, \ a_1^{(-2)} = -0.502998787223958, \ a_2^{(-2)} = 0.161059275050855, \ a_3^{(-2)} = 0.513579806627478, \ a_4^{(-2)} = -0.1716418933139305$ $a_0^{(-3)} = 0, \ a_1^{(-3)} = 0.0865551509384589, \ a_2^{(-3)} = -0.0425064733152697, \ a_3^{(-3)} = -0.0880068218556164, \ a_4^{(-3)} = 0.04395818146707, \ a_3^{(-3)} = 0.0880068218556164, \ a_4^{(-3)} = 0.088006821856164, \ a_4^{(-3)}$ $b_0^{(1)} = 1.012453500459714, b_1^{(1)} = 2.097334374214066, b_2^{(1)} = 1.453742261553123, b_3^{(1)} = 0.4086287367114851,$ $b_4^{(1)} = 0.03976734891271412$ $b_0^{(0)} = 1, \ b_1^{(0)} = 0.8165551541642040, \ b_2^{(0)} = -0.8568739613695883, \ b_3^{(0)} = -0.8366848450375022,$ $b_4^{(0)} = -0.1632602282052145$ $b_0^{(-1)} = 1.000004573170796, \ b_1^{(-1)} = 0.000001616169548, \ b_2^{(-1)} = -1.259174904671002, \ b_3^{(-1)} = 0.0079921241913, \ b_3^{(-1)} = 0.007992$ $b_4^{(-1)} = 0.2511765911393588$ $b_0^{(-2)} = 1.000607685752440, \ b_1^{(-2)} = -0.8116554064634220, \ b_2^{(-2)} = -0.8768673247186090, \ b_3^{(-2)} = 0.8595553398839660, \ b_3^{(-2)} = 0.859555339839600, \ b_3^{(-2)} = 0.8595553398839660, \ b_3^{(-2)} = 0.859555339839600, \ b_3^{(-2)} = 0.859555339839600, \ b_3^{(-2)} = 0.859555339839600, \ b_3^{(-2)} = 0.8595553398839600, \ b_3^{(-2)} = 0.859553989600, \ b_3^{(-2)} = 0.8595533989600, \ b_3^{(-2)} = 0.85955533989600, \ b_3^{(-2)} = 0.859555339896000, \ b_3^{(-2)} = 0.859555339896000, \ b_3^{(-2)} = 0.85955539960000000000000$ $b_4^{(-2)} = -0.1716418933139305$ $b_0^{(-3)} = 1.061535701709146, \ b_1^{(-3)} = -2.202815719388985, \ b_2^{(-3)} = 1.539173929206075, \ b_3^{(-3)} = -0.4394913557492488,$ $b_4^{(-3)} = 0.04395818146707210$

Table 10. Optimized coefficients of a two-sided scheme 31-opt-2-0.5 for M=3 and N=1.

```
41-opt-3-0.6:
                          a_0^{(1)} = 0, \ a_1^{(1)} = -0.2072314848018746, \ a_2^{(1)} = 0.4259961829831501, \ a_3^{(1)} = -0.2894795639340527, \ a_3^{(1)} = -0.2072314848018746, \ a_2^{(1)} = 0.4259961829831501, \ a_3^{(1)} = -0.2894795639340527, \ a_3^{(1)} = -0.2072314848018746, \ a_3^{(1)} = 0.4259961829831501, \ a_3^{(1)} = -0.2894795639340527, \ a_3^{(1)} = -0.2072314848018746, \ a_3^{(1)} = -0.2072314848018746, \ a_3^{(1)} = 0.4259961829831501, \ a_3^{(1)} = -0.2894795639340527, \ a_3^{(1)} = -0.28947956397, \ a_3^{(1)} = -0.28947956397, \ a_3^{(1)} =
                            a_4^{(1)} = 0.07698535219432342, \ a_5^{(1)} = -0.006270493057061551 a_0^{(0)} = 1, \ a_1^{(0)} = -1.057224797042076, \ a_2^{(0)} = -0.6608475885450225, \ a_3^{(0)} = 1.036721249943883,
                                                                    a_4^{(0)} = -0.3525248689380824, \ a_5^{(0)} = 0.03387603365013272
                      a_4^{(-1)} = 0, \ a_1^{(-1)} = 1.967880702853717, \ a_2^{(-1)} = -0.1165714756514110, \ a_3^{(-1)} = -1418756027101672,
                        a_4^{(-1)} = 0.6402459538090958, \ a_5^{(-1)} = -0.07279920402991539 a_0^{(-2)} = 0, \ a_1^{(-2)} = -0.987978478289948, \ a_2^{(-2)} = 0.554838128392867, \ a_3^{(-2)} = 0.930736220982244,
                    a_4^{(-2)} = -0.575442169742026, \ a_5^{(-2)} = 0.07784634075956530 a_0^{(-3)} = 0, \ a_1^{(-3)} = 0.3373714601964230, \ a_2^{(-3)} = -0.246552390567162, \ a_3^{(-3)} = -0.304691540764742,
                                                                   a_4^{(-3)} = 0.255319192837479, \ a_5^{(-3)} = -0.04144673874460764
                 a_{0}^{(-4)} = 0, \ a_{1}^{(-4)} = -0.05281740291624100, \ a_{2}^{(-4)} = 0.04313714338757800, \ a_{3}^{(-4)} = 0.04546966087433870,
                                                              a_4^{(-4)} = -0.04458346016078870, \ a_5^{(-4)} = 0.008794061421886520
             b_0^{(1)} = 1.005963076970462, b_1^{(1)} = 2.266956416632934, b_2^{(1)} = 1.819051918521864, b_3^{(1)} = 0.6601259032819619,
                            b_4^{(1)} = 0.1083378174796312, \ b_5^{(1)} = 0.006270493057061551 b_0^{(0)} = 1, \ b_1^{(0)} = 1.057224797042076, \ b_2^{(0)} = -0.6608475885450225, \ b_3^{(0)} = -1.036721249943883,
                                                                      b_4^{(0)} = -0.3525248689380824, \ b_5^{(0)} = -0.03387603365013272
b_0^{(-1)} = 0.9999999498798146, b_1^{(-1)} = 0.3245425346673150, b_2^{(-1)} = -1.259355874401006, b_3^{(-1)} = -0.4142357478355570,
                                                                      b_4^{(-1)} = 0.2762499336595188, \ b_5^{(-1)} = 0.07279920402991539
b_0^{(-2)} = 0.9732935132831980, b_1^{(-2)} = -0.2137665160888480, b_2^{(-2)} = -1.443649358757065, b_3^{(-2)} = 0.5589475065713520,
                                                                    b_4^{(-2)} = 0.2030212378536270, \ b_5^{(-2)} = -0.07784634075956530
 b_0^{(-3)} = 1.175768369732920, b_1^{(-3)} = -1.419929151027054, b_2^{(-3)} = -0.3921593052700280, b_3^{(-3)} = 0.9710677137296820,
                                                                    b_4^{(-3)} = -0.3663818883316356, \ b_5^{(-3)} = 0.04144673874460764
  b_4^{(-4)} = 0.1312977682769417, \ b_5^{(-4)} = -0.008794061421886520
```

Table 11. Optimized coefficients of a two-sided scheme 41-opt-3-0.6 for M=4 and N=1.

```
51-opt-4-0.8:
                                         a_0^{(1)} = 0, \ a_1^{(1)} = -0.1767398794956751, \ a_2^{(1)} = 0.3948890656191663, \ a_3^{(1)} = -0.3102054841166552,
                                                          a_4^{(1)} = 0.1060950140568273, \ a_5^{(1)} = -0.01419469891182375, \ a_6^{(1)} = 0.0001559837806004457
                                                a_0^{(0)} = 1, \ a_1^{(0)} = -1.236283089901758, \ a_2^{(0)} = -0.4.77569579896645, \ a_3^{(0)} = 1.158963892100039,
                                                     a_4^{(0)} = -0.5.269997846949658, \ a_5^{(0)} = 0.08.390301503827131, \ a_6^{(0)} = -0.002.014458050832157131, \ a_6^{(0)} = -0.002.0144580508321131, \ a_6^{(0)} = -0.002.014458050831131, \ a_6^{(0)} = -0.002.014458050801111, \ a_6^{(0)} = -0.002.0144111, \ a_6^{(0)} = -0.002.01411111, \ a_6^{(0)} = -0.002.0141
                                     a_0^{(-1)} = 0, \ a_1^{(-1)} = 2.415846975277249, \ a_2^{(-1)} = -0.5.771547514709360, \ a_3^{(-1)} = -1.7250705320837,
                                                     a_4^{(-1)} = 1.085240379289086, \ a_5^{(-1)} = -0.2.065945915140004, \ a_6^{(-1)} = 0.007.732533545154094
                                        a_0^{(-2)} = 0, \ a_1^{(-2)} = -1.599092745511250, \ a_2^{(-2)} = 1.186533492466867, \ a_3^{(-2)} = 1.348086223000850,
                                                       a_4^{(-2)} = -1.192863951343233, \ a_5^{(-2)} = 0.2712421939097631, \ a_6^{(-2)} = -0.01390522928430374
                                         a_0^{(-3)} = 0, \ a_1^{(-3)} = 0.816125476322960, \ a_2^{(-3)} = -0.74431215389603, \ a_3^{(-3)} = -0.63039213575091,
                                                             a_4^{(-3)} = 0.74572221439243, \ a_5^{(-3)} = -0.2002686993506443, \ a_6^{(-3)} = 0.01312531038130151
                                        a_0^{(-4)} = 0, \ a_1^{(-4)} = -0.25650589073832, \ a_2^{(-4)} = 0.2561563420434330, \ a_3^{(-4)} = 0.183221175033803,
                                    a_{4}^{(-4)} = -0.2553852527776407, \ a_{5}^{(-4)} = 0.0788423013075866, \ a_{6}^{(-4)} = -0.006328679519750083 a_{0}^{(-5)} = 0, \ a_{1}^{(-5)} = 0.036649154046801, \ a_{2}^{(-5)} = -0.0385424148658540, \ a_{3}^{(-5)} = -0.02460313818343,
                                                 a_4^{(-5)} = 0.03819138107749597, \ a_5^{(-5)} = -0.01292952047915256, \ a_6^{(-5)} = 0.00123453914782992866 + 0.0012345391478299286 + 0.0012345391478299286 + 0.001234539147829928 + 0.001234539147829928 + 0.001234539147829928 + 0.001234539147829928 + 0.001234539147829928 + 0.001234539147829928 + 0.001234539147829928 + 0.001234539147829928 + 0.001234539147829928 + 0.001234539147829928 + 0.001234539147829928 + 0.001234539147829928 + 0.001234539147829928 + 0.001234539147829928 + 0.001234539147829928 + 0.001234539147829928 + 0.001234539147829928 + 0.001234539147829928 + 0.001234539147829928 + 0.001234539147829928 + 0.001234539147829928 + 0.001234539147829928 + 0.001234539147829928 + 0.001234539147829928 + 0.001234539147829928 + 0.001234539147829928 + 0.001234539147829928 + 0.001234539147829928 + 0.001234539147829928 + 0.0012345391478 + 0.0012345391478 + 0.0012345391478 + 0.0012345391478 + 0.0012345391478 + 0.0012345391478 + 0.001234579 + 0.001234579 + 0.001234579 + 0.001234579 + 0.001234579 + 0.001234579 + 0.001234579 + 0.001234579 + 0.001234579 + 0.001234579 + 0.001234579 + 0.001234579 + 0.001234579 + 0.001234579 + 0.001234579 + 0.001234579 + 0.001234579 + 0.001234579 + 0.001234579 + 0.001234579 + 0.001234579 + 0.001234579 + 0.001234579 + 0.001234579 + 0.001234579 + 0.001234579 + 0.001234579 + 0.001234579 + 0.001234579 + 0.001234579 + 0.001234579 + 0.001234579 + 0.001234579 + 0.001234579 + 0.001234579 + 0.001234579 + 0.001234579 + 0.001234579 + 0.001234579 + 0.001234579 + 0.001234579 + 0.001234579 + 0.001234579 + 0.00123479 + 0.00123479 + 0.00123479 + 0.00123479 + 0.00123479 + 0.00123479 + 0.00123479 + 0.00123479 + 0.00123479 + 0.00123479 + 0.00123479 + 0.00123479 + 0.00123479 + 0.00123479 + 0.00123479 + 0.00123479 + 0.00123479 + 0.00123479 + 0.00123479 + 0.00123479 + 0.00123479 + 0.00123479 + 0.00123479 + 0.00123479 + 0.00123479 + 0.00123479 + 0.00123479 + 0.00123479 + 0.00123479 + 0.00123479 + 0.00123479 + 0.00123479 + 0.00123479 + 0.00123479 + 0.00123479 + 0.00123479 + 0.0012479 + 0.0012479 + 0.0012479 + 0.00
                   b_0^{(1)} = 1.002280125980748, \ b_1^{(1)} = 2.393423916554004, \ b_2^{(1)} = 2.106362348137340, \ b_3^{(1)} = 0.8.796522050742108, \ b_3^{(1)} = 0.8.79652200742108, \ b_3^{(1)} = 0.8.79652200742108, \ b_3^{(1)} = 0.8.79652007420000000000000000000000000000000
                                                           b_4^{(1)} = 0.1.794082653249527, \ b_5^{(1)} = 0.01.513060159542642, \ b_6^{(1)} = 0.0001.559837806004457
                                                  b_0^{(0)} = 1, b_1^{(0)} = 1.236283089901758, b_2^{(0)} = -0.477569579896645, b_3^{(0)} = -1.158963892100039,
                                                     b_4^{(0)} = -0.5269997846949658, \ b_5^{(0)} = -0.08390301503827131, \ b_6^{(0)} = -0.00201445805083215711, \ b_6^{(0)} = -0.0020144580508321571, \ b_6^{(0)} = -0.0020144580508321, \ b_6^{(0)} = -0.00201445801, \ b_6^{(0)} 
b_0^{(-1)} = 1.000000013042853, b_1^{(-1)} = 0.559290363058456, b_2^{(-1)} = -1.190881983950213, b_3^{(-1)} = -0.7045957408357219,
                                                           b_4^{(-1)} = 0.1682554248963954, b_5^{(-1)} = 0.1601993902430758, b_6^{(-1)} = 0.007732533545154094
b_0^{(-2)} = 1.03663057227702, \ b_1^{(-2)} = -0.1.8200094757769, \ b_2^{(-2)} = -0.9.91563517217471, \ b_3^{(-2)} = -0.4.30025683156908,
                                                 b_4^{(-2)} = 0.6.852442306961736, \ b_5^{(-2)} = -0.1.043794424981182, \ b_6^{(-2)} = -0.01.390522928430374
             b_0^{(-3)} = 0.035536070179111, \ b_1^{(-3)} = 2.10445665901869, \ b_2^{(-3)} = -4.27413850985563, \ b_3^{(-3)} = 2.618240898696925
                                                        b_4^{(-3)} = -0.48639137439153, b_5^{(-3)} = -0.0359868875127829, b_6^{(-3)} = 0.01312531038130151
            b_0^{(-4)} = 4.23225362690136, \ b_1^{(-4)} = -7.24347524052195, \ b_2^{(-4)} = 4.09476965681066, \ b_3^{(-4)} = -0.611115554525306
                                                   b_4^{(-4)} = -0.197422311365929, b_5^{(-4)} = 0.0730460071664154, b_6^{(-4)} = -0.006328679519750083
      b_0^{(-5)} = -1.101171013415250, \ b_1^{(-5)} = 0.355462295161609, \ b_2^{(-5)} = 0.73302158597198, \ b_3^{(-5)} = -0.593192233153169
                                                       b_4^{(-5)} = 0.177905549534905, b_5^{(-5)} = -0.02410665395574528, b_6^{(-5)} = 0.001234539147829928
```

Table 12. Optimized coefficients of a two-sided scheme 51-opt-4-0.8 for M=5 and N=1.

#### References

- <sup>1</sup>Warren F. Ahtye and Geraldine McCulley, Evaluation of Approximate Methods for the Prediction of Noise Shielding by Airframe Components, NASA Technical Paper 1004, 1980.
- $^{2}$ L. Banjai, Multistep and multistage boundary integrals for the wave equation, Max-Planck Institute Preprint No. 58, 2010
- <sup>3</sup>A. Boag, V. Lomakin and E Michielssen, Non-uniform grid time domain (NGTD) algorithm for fast evaluation of transient fields, IEEE trans. Antennas Propag., Vol. 54, 1943-1951, 2006.
- <sup>4</sup>Y. Brick and A. Boag, "Multilevel nonuniform grid algorithm for acceleration of integral equation-based solvers for acoustic scattering", IEEE transaction on ultrasonic, ferroelectrics, and frequency control, Vol. 57, 261-273, 2010
- <sup>5</sup>O. M. Bucci, and G. Franceschetti, On the spatial bandwidth of scattered fields, IEEE Trans. Antennas Propag., Vol. 35, 1445-1455, 1987.
- <sup>6</sup>A. J. Burton and G. F. Miller, The application of integral equation methods to the numerical solution of some exterior boundary-value problems, Proc.R.Soc.London, Ser A, Vol. 323, 201-210, 1971.
- <sup>7</sup>D. J. Chappell, P. J. Harris, D. Henwood and R. Chakrabarti, "A stable boundary element method for modeling transient acoustic radiation", Journal of Acoustical Society of America, Vol. 120, No. 1, 74-80, 2006.
- <sup>8</sup>D. J. Chappell, Convolution quadrature Galerkin boundary element method for the wave equation with reduced quadrature weight computation, IMA Journal of Numerical Analysis, doi:10.1093/imanum/drp045, 2010.
- <sup>9</sup>M. Costabel, "Time-dependent problems with boundary integral equations", Encyclopedia of Computational Mechnics, E. Stein, R. de Borst and T. J. R. Hughes eds, John Wiley & Sons, 2004.
- <sup>10</sup>A. A. Ergin, B. Shanker and E. Michielssen, "Analysis of transient wave scattering from rigid bodies using a Burton-Miller approach", Journal of Acoustical Society of America, Vol. 106, No. 5, 2396-2404, 1999.
- <sup>11</sup>A. A. Ergin, B. Shanker and E. Michielssen, "Fast analysis of transient acoustic wave scattering from rigid bodies using the multilevel plane wave time domain algorithm", Journal of Acoustical Society of America, Vol. 107, No. 3, 1168-1178, 2000.
- <sup>12</sup>A. Geranmayeh, W. Ackermann and T. Weiland, "Temporal discretization choices for stable boundary element methods in electromagnetic scattering problems", Applied numerical mathematics, Vol. 59, 2751-2773, 2009.
- <sup>13</sup>L. Greengard and V. Rokhlin, "A fast algorithm for particle simulations", Journal of Computational Physics, Vol. 135, 280-292, 1997.
- <sup>14</sup>N. A. Gumerov and R. Duraiswami, Fast Multipole methods for the Helmholtz equations in three dimensions, Elsevier, 2004.
- <sup>15</sup>N. A. Gumerov and R. Duraiswami, "A broadband fast multipole accelerated boundary element method for the three dimensional Helmholtz equation", Journal of Acoustical Society of America, Vol. 125, 191-205, 2009.
- <sup>16</sup>N. A. Gumerov and R. Duraiswami, Fast multipole methods on graphics processors, Journal of Computational Physics, Vol. 227, 8290-8313, 2008.
- <sup>17</sup>T Ha-Duong, B. Ludwig and I. Terrasse, A Galerkin BEM for transient acoustic scattering by an obstacle, Int. J. Numer. Meth. Eng., Vol. 57, 1845-1882, 2003.
- <sup>18</sup>W. Hackbusch, W. Kress and S. Sauter, Sparse convolution quadrature for time domain boundary integral formulations of the wave equation, IMA Journal of Numer. Anal., Vol. 29, 158-179, 2009
- <sup>19</sup>F. Q. Hu, An efficient solution of time domain boundary integral equations for acoustic scattering and its acceleration by Graphics Processing Units, AIAA 2013-2018, 2013.
- <sup>20</sup>A. D. Jones and F. Q. Hu, "A three-dimensional time-domain boundary element method for the computation of exact Green's functions in acoustic analogy", AIAA paper 2007-3479, 2007.
- <sup>21</sup>D. P. Lockard, An efficient, two-dimensional implementation of the Ffowcs Williams and Hawkings equation, Journal of Sound and Vibration, Vol. 229, 897-911, 2000.
- <sup>22</sup>S. Li, B. Livshitz and V. Lomakin, "Fast evaluation of Helmholtz potential on graphics processing units (GPUs)", Journal of Computational Physics, Vol. 229, 8463-8438, 2010.
- <sup>23</sup>S. Li, B. Livshitz and V. Lomakin, Graphics Processing Unit accerelated O(N) micromegnetic solver, IEEE Transactions on Magnetics, Vol. 46, No. 6, 2373-2375, 2010.
- <sup>24</sup>Ch. Lubich, Convolution quadrature and discretized operational calculus. I, Numer. Math., Vol. 52, 129-145, 1988.
  <sup>25</sup>Ch. Lubich, On the multistep time discretization of linear initial boundary value problems and their boundary integral equations, Numer. Math., Vol. 67, 365-389, 1994.
- <sup>26</sup>J. Meng, A. Boag, V. Lomakin and E. Michielssen, "A multi-level Cartesian non-uniform grid time domain algorithm", Journal of Computational Physics, Vol. 229, 8430-8444, 2010
- <sup>27</sup>A. Shlivinski and A. Boag, Multilevel surface decomposition algorithm for rapid evaluation of transient near-field to far-field transforms, IEEE Transaction of Antennas and Propagation, Vol. 57, 188-195, 2009.

- <sup>28</sup>J. C. Strikwerda, Finite Difference Schemes and Partial Differential Equations, SIAM, 2004.
- <sup>29</sup>C. K. W. Tam and F. Q. Hu, An optimized multi-dimensional interpolation scheme for computational aeroacoustics applications using overset grids, AIAA paper 2004-2812, 2004.
- <sup>30</sup>C. K. W. Tam and K. Kurbatskii, "A Wavenumber Based Extrapolation and Interpolation Method for Use in Conjunction with High-Order Finite Difference Schemes", Journal of Computational Physics, Vol. 157, 588–617, 2000.
- <sup>31</sup>X. Wang and D. S. Weile, Implicit Runge-Kutta Methods for the discretization of time domain integral equations, IEEE Transactions on Antennas and Propagation, Vol. 59, 4651-4663, 2011.
- <sup>32</sup>E. van't Wout, D. R. van der Heul, H. van der Ven and C. Vuik, Design of temporal basis functions for time domain integral equation methods with predefined accuracy and smoothness, IEEE Transactions on Antennas and Propagation, Vol. 61, 271-280, 2013.
- <sup>33</sup>D. S. Weile, G. Pisharody, N.-W. Chen, B. Shanker and E. Michielssen, A novel scheme for the solution of the time-domain integral equations of electromagnetics, IEEE Transactions on Antennas and Propagation, Vol. 52, 283-295, 2004.